

**CASE FILE
COPY**

N 62 70070

NASA MEMO 12-3-58A

NASA

MEMORANDUM

LARGE-SCALE WIND-TUNNEL TESTS OF AN AIRPLANE MODEL

WITH AN UNSWEPT, ASPECT-RATIO-10 WING,

TWO PROPELLERS, AND BLOWING FLAPS

By Roy N. Griffin, Jr., Curt A. Holzhauser,
and James A. Weiberg

Ames Research Center
Moffett Field, Calif.

**NATIONAL AERONAUTICS AND
SPACE ADMINISTRATION**

WASHINGTON

December 1958

NATIONAL AERONAUTICS AND SPACE ADMINISTRATION

MEMORANDUM 12-3-58A

LARGE-SCALE WIND-TUNNEL TESTS OF AN AIRPLANE MODEL

WITH AN UNSWEPT, ASPECT-RATIO-10 WING,

TWO PROPELLERS, AND BLOWING FLAPS

By Roy N. Griffin, Jr., Curt A. Holzhauser,
and James A. Weiberg

SUMMARY

An investigation was made to determine the lifting effectiveness and flow requirements of blowing over the trailing-edge flaps and ailerons on a large-scale model of a twin-engine, propeller-driven airplane having a high-aspect-ratio, thick, straight wing.

With sufficient blowing jet momentum to prevent flow separation on the flap, the lift increment increased for flap deflections up to 80° (the maximum tested). This lift increment also increased with increasing propeller thrust coefficient. The blowing jet momentum coefficient required for attached flow on the flaps was not significantly affected by thrust coefficient, angle of attack, or blowing nozzle height.

INTRODUCTION

This report presents the results of an investigation which was made to study the lifting effectiveness and flow requirements of blowing boundary-layer control applied to the trailing-edge flaps and ailerons of a powered model of a propeller-driven, twin-engine, straight-wing airplane. The model, with the exception of the boundary-layer-control system, was identical to that used for the area-suction boundary-layer-control studies reported in reference 1. The design of the boundary-layer-control system of the model was based on the studies presented in reference 2.

In the investigation, tests were made to determine: (1) the aerodynamic effects and flow requirements of boundary-layer control for a range of flap and aileron deflections at various thrust coefficients, (2) the effect of a simulated leading-edge flap on maximum lift, (3) the extent to which jet momentum coefficient remained a correlating parameter for boundary-layer control in the presence of the propeller slipstream, and (4) the effectiveness of differentially deflected drooped ailerons with boundary-layer control as a means of lateral control.

The study was made in the 40- by 80-foot wind tunnel of the Ames Aeronautical Laboratory. Test Reynolds numbers based on wing mean aerodynamic chord were from 2.0 million to 2.6 million.

NOTATION

b	wing span, ft
c	local wing chord parallel to plane of symmetry, ft
\bar{c}	mean aerodynamic chord, $\frac{2}{S} \int_0^{b/2} c^2 dy$, ft
C_D'	drag coefficient, $C_D + T_C'$
C_D	drag coefficient, including thrust, $\frac{\text{measured drag}}{q_\infty S}$
C_L	lift coefficient, $\frac{\text{lift}}{q_\infty S}$
ΔC_L	increment of lift coefficient
C_l	rolling-moment coefficient, $\frac{\text{rolling moment}}{q_\infty S b}$
C_m	pitching-moment coefficient, $\frac{\text{pitching moment}}{q_\infty S \bar{c}}$
C_n	yawing-moment coefficient, $\frac{\text{yawing moment}}{q_\infty S b}$
C_Y	lateral-force coefficient, $\frac{\text{lateral force}}{q_\infty S}$
C_μ	jet momentum coefficient, $\frac{W_j/g}{q_\infty S} V_j$
D	propeller diameter, ft
g	acceleration of gravity, 32.2 ft/sec ²
h_j	nozzle height, in.
i_t	angle of stabilizer setting (relative to fuselage reference line), deg
J	propeller advance ratio, $\frac{U_\infty}{nD}$
n	propeller angular velocity, rps

p	static pressure, lb/sq ft
p _d	total pressure in flap duct, lb/sq ft
q	dynamic pressure, lb/sq ft
R	gas constant for air, 1715 sq ft/sec ² °R
S	wing area, sq ft
T _d	air temperature in duct, °R
T _C '	thrust coefficient, $\frac{\text{thrust}}{q_{\infty} S}$
U	velocity, ft/sec
V _j	jet velocity assuming isentropic expansion, $\sqrt{\frac{2\gamma}{\gamma-1} RT_d \left[1 - \left(\frac{p_{\infty}}{p_d} \right)^{\frac{\gamma-1}{\gamma}} \right]}, \text{ ft/sec}$
W _j	weight rate of flow through nozzle, lb/sec
w	specific weight of air at standard conditions, 0.0765 lb/cu ft
y	spanwise distance perpendicular to plane of symmetry, ft
α	angle of attack of fuselage reference line, deg
δ	deflection of flap or aileron measured normal to hinge line, deg
Δδ _a	total deflection of right and left ailerons, deg
γ	ratio of specific heats, 1.4 for air

Subscripts

a	aileron
d	duct
f	flap
L	left
max	maximum

R	right
u	uncorrected
∞	free stream

MODEL AND APPARATUS

The geometry of the model is shown in figure 1, and a photograph of the model mounted in the wind tunnel is shown in figure 2. Pertinent dimensions of the model are listed in table I.

The propellers and the variable-speed electric motors and reduction gears used to drive the propellers were the same as those described in reference 1.

Blowing Nozzle Arrangement

Details of the flaps and ailerons as well as the location of the boundary-layer-control jet nozzle are shown on the cross-section view in figure 3. The jet-nozzle location on the flaps and ailerons was selected on the basis of the results of the blowing boundary-layer-control application presented in reference 2. The nozzle height was adjustable.

Boundary-Layer-Control Blowing System

The air for boundary-layer control was supplied by a centrifugal compressor driven by a variable-speed electric motor. The maximum compressor pressure ratio used during the test was 1.65. The compressed air flowed from the compressor to a plenum chamber. Separate ducts were used to transmit the compressed air from the plenum chamber into each of the flaps and ailerons. Each of these ducts contained a thin-plate orifice meter with pressure orifices and a thermocouple for measuring the pressures and temperature required for determining the boundary-layer-control flow and jet momentum coefficients. The air flow to each of the flaps and ailerons was controlled by electrically actuated butterfly valves located within the ducts.

TESTS

Longitudinal force and moment measurements were made through a range of angles of attack at 0° angle of sideslip with flap deflections of 0° , 40° , 60° , and 80° , and symmetrical aileron deflections of 0° , 30° , and 50° for various values of thrust coefficient, T_C' .

Tests were made with varying boundary-layer-control jet momentum coefficients applied to the flaps and ailerons at constant angle of attack for several values of thrust coefficient. This was done to determine the effect of jet momentum coefficient on lift coefficient for various flap deflections, and to determine if the jet momentum coefficient requirements for boundary-layer control varied with thrust coefficient.

Tests were made with varying flap jet momentum coefficient at constant angle of attack and thrust coefficient for several values of nozzle height, h_j . These tests were made to determine if jet momentum coefficient is the significant parameter for boundary-layer control on a flap which is immersed in a propeller slipstream. With the exception of these tests to determine the effect of varying h_j , all of the tests reported herein were made with $h_j = 0.040$ inch.

The simulated nose flap shown in figure 3 was attached to the wing leading edge along the entire wing span, and some tests were made to study the aerodynamic characteristics of the model to higher values of maximum lift than could be reached by the model with the plain leading edge.

Lateral control tests for several values of differential aileron deflection were made by moving the model through a range of angle of attack at 0° angle of sideslip and with boundary-layer control applied. Tests were also made with varying momentum coefficient to the downward deflected aileron to establish the momentum coefficient requirements for various aileron deflections.

The propeller thrust calibration was made with the flaps and ailerons undeflected and with the model set at the angle of attack for zero lift. It was assumed that the propeller thrust was equal to the sum of the measured thrust and the measured drag of the model with propellers removed. Figure 4 shows the variation of total-thrust coefficient with advance ratio at two wind-tunnel airspeeds for the blade angle setting used throughout the test. For setting thrust coefficient the propeller rotational speed was set constant, and it was assumed that there was no variation of thrust with inflow angle. The propeller rotational velocity was set to the predetermined values for each test by visually matching on an oscilloscope the propeller driving motor speed (from a tachometer) against the output from a signal generator.

The drag coefficients presented in this report are the algebraic sum of the measured drag coefficients plus the thrust coefficient. It was assumed that $T_C' \cos \alpha = T_C'$. It should also be noted that the lift coefficients include $T_C' \sin \alpha$.

The following tunnel-wall corrections were applied to the angle of attack, drag coefficient, and pitching-moment coefficient data.

$$\alpha = \alpha_u + 0.41 C_L$$

$$C_D = C_{D_u} + 0.0073 C_L^2$$

$$C_m = C_{m_u} + 0.0147 C_L \text{ (tail-on data only)}$$

There were no tare corrections applied for strut interference as their values were not known.

RESULTS AND DISCUSSION

Lift, Drag, and Pitching-Moment Characteristics of the Model

Presentation of results.— Figures 5 and 6 show the lift, drag, and pitching-moment characteristics of the model for various deflections of flaps and ailerons at several fixed values of T_C' . For the data shown in figure 5 with boundary-layer control applied, the jet momentum coefficient C_μ on the flaps was held slightly above the minimum required to maintain attached flow to the flaps. The flow over the flaps and ailerons was considered to be attached when, by visual observation, the upper-surface trailing-edge pressures on a manometer board showed little or no change with increased jet momentum coefficient. The data of figure 6 were obtained with increased momentum coefficient applied to the 60° and 80° flap deflections. For the data in both figures, the momentum coefficient applied to the ailerons was held slightly above the minimum required to maintain attached flow to the ailerons.

Observations of the static pressure distributions showed that flow separation was occurring near the leading edge of the wing slightly outboard of the propeller, and was limiting $C_{L_{max}}$. For this reason, the simulated leading-edge flap (see fig. 3) was installed. The lift, drag, and pitching-moment characteristics of the model with this leading-edge flap are shown in figure 7 for flap deflections of 60° and 80°. These data are presented with flap jet momentum coefficient required for flow attachment and also with higher values of flap jet momentum coefficient.

It should be pointed out that the horizontal tail was stalled during some of the tests.

Lift at 0° angle of attack.- The variation of lift coefficient at 0° angle of attack is shown in figure 8 as a function of flap deflection for three values of flap jet momentum coefficient, $C_{\mu f}$, and three values of thrust coefficient, T_C' . Also shown is a prediction of the lift due to flap deflection without propellers as obtained by the method of reference 3.

It is evident that if the $C_{\mu f}$ is limited to that required to maintain essentially attached flow at the flap trailing edge (as observed from pressure distributions) theoretical flap lift for propellers off is realized at the lowest T_C' . It is further evident that within the range studied, the individual effects of T_C' and $C_{\mu f}$ (above that required for boundary-layer control) on lift are at least additive; that is, an increase in $C_{\mu f}$ gives essentially the same increase in lift coefficient at low T_C' as at high T_C' , and an increase in T_C' gives essentially the same increase in lift coefficient at low C_{μ} as at high C_{μ} .

The variation of lift coefficient with T_C' at 0° angle of attack is shown in figure 9 for several flap deflections with C_{μ} sufficient for attached flow only. Also shown is the predicted variation of lift coefficient with T_C' based on the slipstream velocity. These predicted values were obtained by the method of reference 4, as described in reference 1. As was true in the latter case, theory gives a reasonable prediction of the effect of T_C' when attached flow is maintained on the flap.

Maximum lift.- The effects on maximum lift coefficient of increasing T_C' , increasing flap deflection, and increasing C_{μ} , and of a simulated leading-edge flap are summarized in figure 10. It can be seen that within the ranges studied each one of these variables had a significant effect on maximum lift. It is further apparent that increases in $C_{L_{max}}$ result from using all of these variables in combination. For no case tested did it appear that any one parameter had its value increased to such a point that it canceled the effectiveness of any other parameter. The effectiveness of the simulated leading-edge flap is of particular interest since, as was the case in reference 1, the angle of attack for $C_{L_{max}}$ was increased 4° to 5° for each condition studied. Therefore, it is concluded that without the nose flap leading-edge air-flow separation had limited the maximum lift. It should be noted that the basic wing area, 205.4 sq ft, was also used in calculating the aerodynamic coefficients of the model with the nose flap.

Effect of stabilizer incidence.- Figures 11(a) through 11(c) show the effect of varying stabilizer incidence on the longitudinal characteristics of the model at several values of thrust coefficient. For these tests ($\delta_f = 60^\circ$, $\delta_a = 30^\circ$), the momentum coefficient to the flaps and ailerons was about the minimum required to prevent air-flow separation.

Tail-off data are also included to indicate the magnitude of the horizontal tail load. The dotted portions of the pitching-moment curves shown in figures 11(a) through 11(c) represent the region where the horizontal tail was believed to have been stalled.

Lateral Control With Drooped Ailerons

The effectiveness of the ailerons differentially deflected from drooped and undrooped positions is shown in figures 12(a) through 12(c) for several values of T_C' . It is evident that, with boundary-layer control applied to the drooped ailerons, lateral control is maintained to $C_{L_{max}}$ and is equal to or greater than that value for undrooped ailerons of equal total differential deflection.

Figure 13 compares experimental and theoretical values of rolling-moment coefficient as a function of total differential aileron deflection. The theoretical values were computed by the method of reference 5. The theoretical value of $d\alpha/d\delta$ for this aileron chord ratio was used in the computation. It can be seen that the ailerons with boundary-layer control applied exceeded theoretical values of rolling-moment coefficient. The value of C_{μ_a} for all deflections exceeded somewhat the minimum values required for attached flow.

Figure 14 shows yawing-moment coefficient as a function of rolling-moment coefficient for the undrooped and drooped ailerons of various differential deflections with boundary-layer control applied.

Effect of Variation of Jet Momentum Coefficient

Effect of flap jet momentum coefficient on lift coefficient.— The effect of flap momentum coefficient on lift coefficient for various values of flap deflection and thrust coefficient is presented in figure 15. It is not evident from these curves precisely what value of C_{μ_f} is required to keep the flow attached to the flap since there is, in general, no distinct flattening of the curve to a sensibly constant slope as is found with area-suction boundary-layer control. Visual observation of the wing static pressure distributions aided in determining the values of C_{μ_f} required for flow attachment. These values are ticked on the curves of figure 15, and are summarized below.

δ_f , deg	C_{μ_f} required
40	0.03
60	.035
80	.05

It is interesting to note that while the values of C_{μ_f} were functions of flap deflection, they were not significantly affected by thrust coefficient or angle of attack within the range of variables tested.

Effect of nozzle height.- Figure 16 shows the effect of C_{μ_f} on lift coefficient for four values of jet nozzle height from 0.020 inch to 0.050 inch. It is evident that, within the range of experimental error, for a given value of C_{μ_f} , lift coefficient is independent of nozzle height, and C_{μ} is the correlating parameter for boundary-layer control.

Effect of aileron jet momentum coefficient on lift and rolling-moment coefficient.- Figure 17 shows that for a symmetrical aileron deflection of 30° , the minimum value of C_{μ_a} required for boundary-layer control is of the order of 0.003. As in the flap case, the C_{μ_a} required is independent of angle of attack. These tests were made with the flaps deflected 60° and with boundary-layer control applied to the flaps.

Figure 18 shows the effect on lift coefficient and rolling-moment coefficient of applying boundary-layer control to the more highly deflected aileron. Values of C_{μ_a} required for flow attachment have been marked by ticks on the curves. It is seen that both aerodynamic coefficients continue to increase with increasing C_{μ_a} as did the flap lift increment.

CONCLUDING REMARKS

The results of the wind-tunnel investigation indicate that with sufficient jet momentum to prevent air-flow separation, the lift coefficient developed increased with increasing flap deflection up to at least 80° , and also increased with increasing thrust coefficient.

The momentum coefficient requirements for attached flow on the deflected flaps varied from about 0.030 for the 40° deflection to about 0.055 for the 80° deflection. Neither thrust coefficient nor angle of attack had any significant effect on the momentum coefficient requirements for boundary-layer control at angles of attack below the stall.

The addition of a simulated leading-edge flap allowed the model to reach angles of attack 5° to 6° higher than the model with the plain leading edge before stall occurred.

The use of differentially deflected drooped ailerons with boundary-layer control applied gave substantial rolling moments up to the maximum lift coefficient of the model.

Ames Research Center

National Aeronautics and Space Administration
Moffett Field, Calif., Aug. 26, 1958

REFERENCES

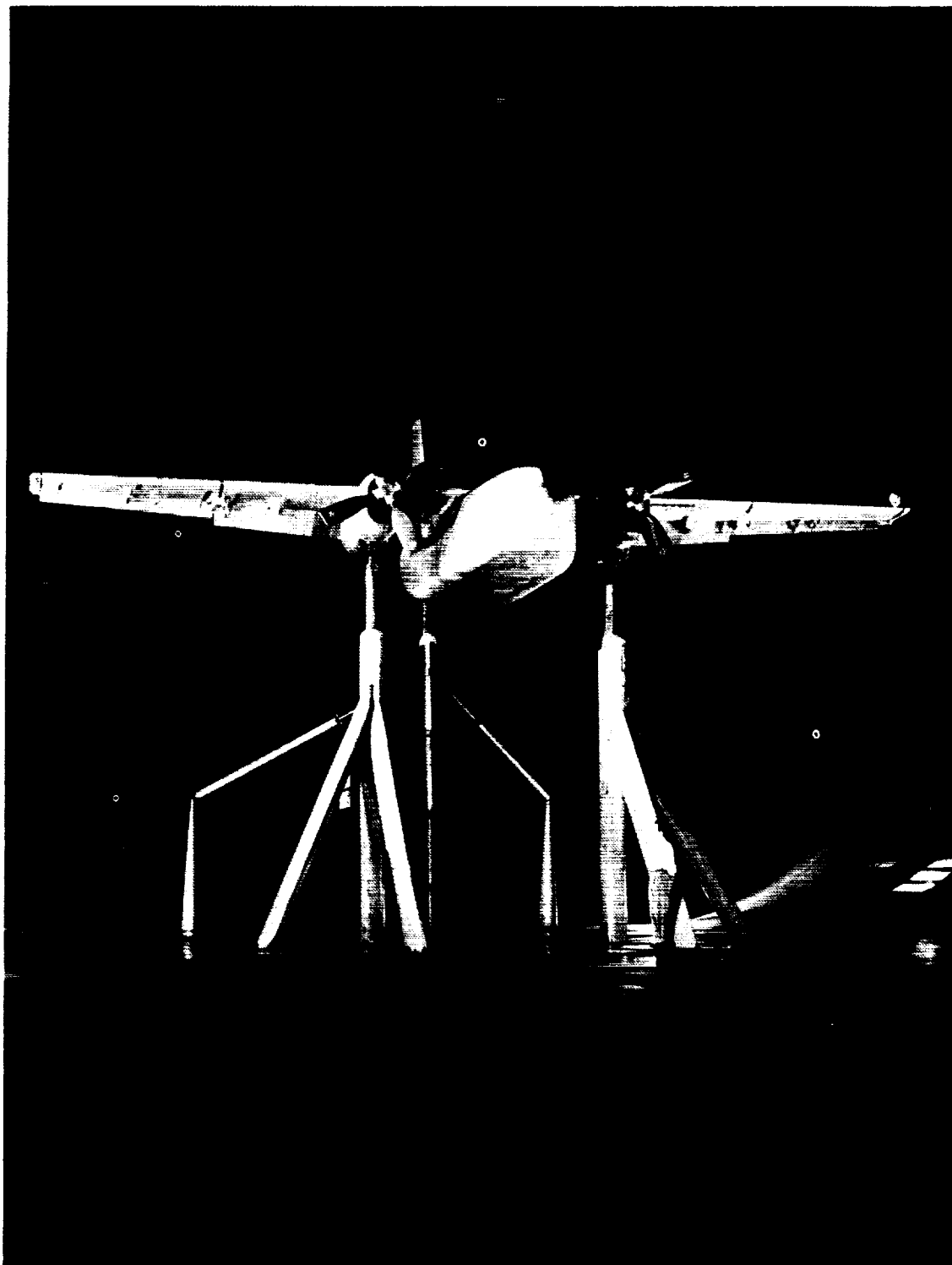
1. Weiberg, James A., Griffin, Roy N., Jr., and Florman, George L.: Large-Scale Wind-Tunnel Tests of an Airplane Model With an Unswept, Aspect-Ratio-10 Wing, Two Propellers, and Area-Suction Flaps. NACA TN 4365, 1958.
2. Kelly, Mark W., and Tolhurst, William H., Jr.: Full-Scale Wind-Tunnel Tests of a 35° Sweptback Wing Airplane With High-Velocity Blowing Over the Trailing-Edge Flaps. NACA RM A55IO9, 1955.
3. DeYoung, John: Theoretical Symmetric Span Loading Due to Flap Deflection for Wings of Arbitrary Plan Form at Subsonic Speeds. NACA Rep. 1071, 1952.
4. Smelt, R., and Davies, H.: Estimation of Increase in Lift Due to Slipstream. R. & M. 1788, British, 1937.
5. DeYoung, John: Theoretical Antisymmetric Span Loading for Wings of Arbitrary Plan Form at Subsonic Speeds. NACA Rep. 1056, 1951.

TABLE I.- GENERAL GEOMETRIC DIMENSIONS OF THE MODEL

Dimension ¹	Wing	Horizontal surface	Vertical surface
Area, sq ft	205.4	56.5	30.6
Span, ft	45.00	16.03	7.19
M.A.C., ft	4.73	3.50	4.68
Aspect ratio	9.86	4.55	1.69
Taper ratio	.50	.45	.55
Geometric twist, deg	4.8 ^o (washout)	0	0
Dihedral from reference plane, deg	0.8	0	---
Incidence from reference plane, deg	8.3	---	---
Section profile (constant)	NACA 23017	NACA 63-012	NACA 0012
Root chord, ft	6.07	4.61	5.88
Tip chord, ft	3.06	2.54	2.65
Sweep of leading edge, deg	2	12	24
Tail length, ft	---	² 18.01	---

¹Propeller dimensions are given in reference 1.

²Distance from quarter chord of wing to quarter chord of horizontal tail.



A-22323

Figure 2.- Photograph of the model mounted in the Ames 40- by 80-foot wind tunnel.

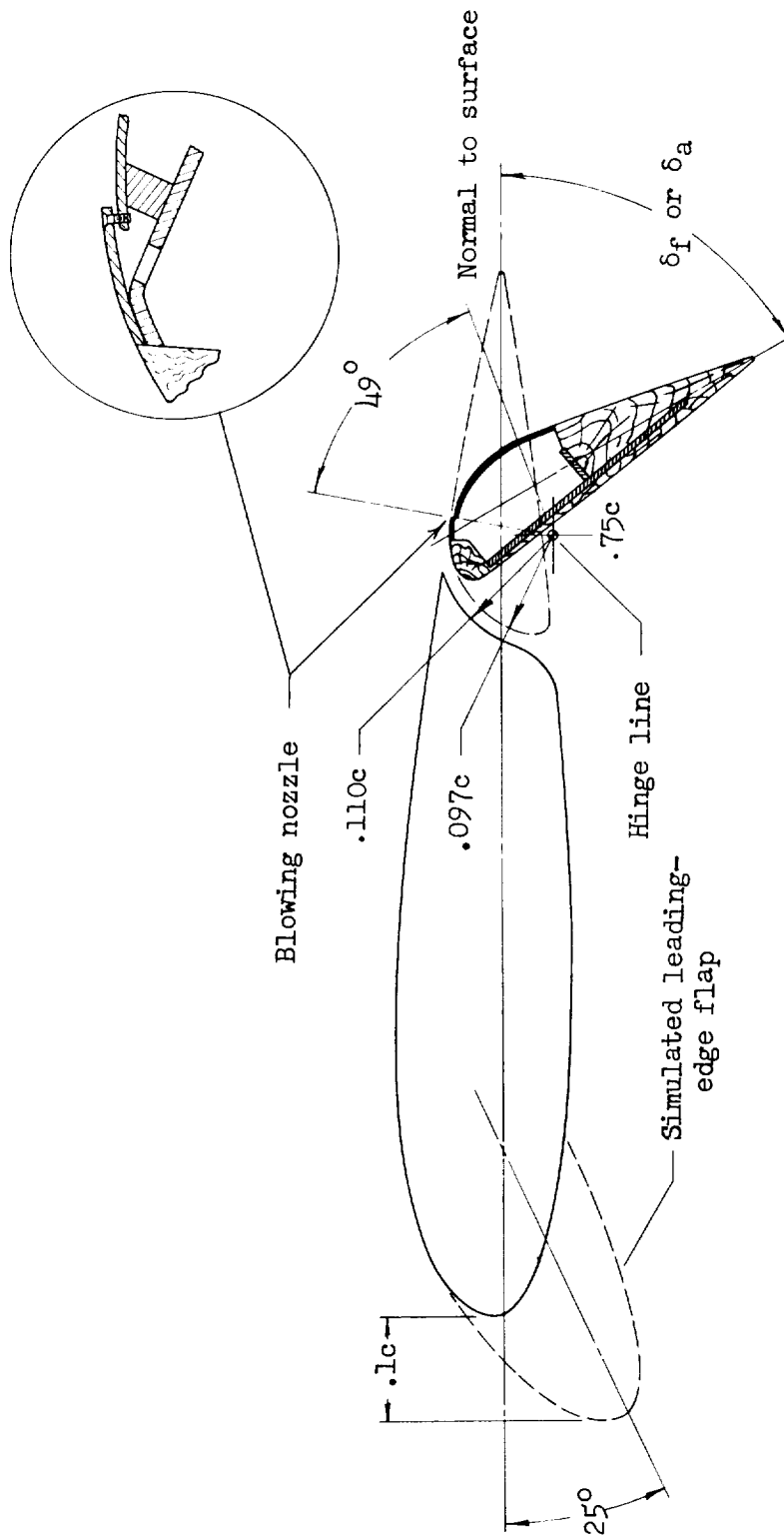


Figure 3.- Details of flaps, ailerons, and simulated nose flap.

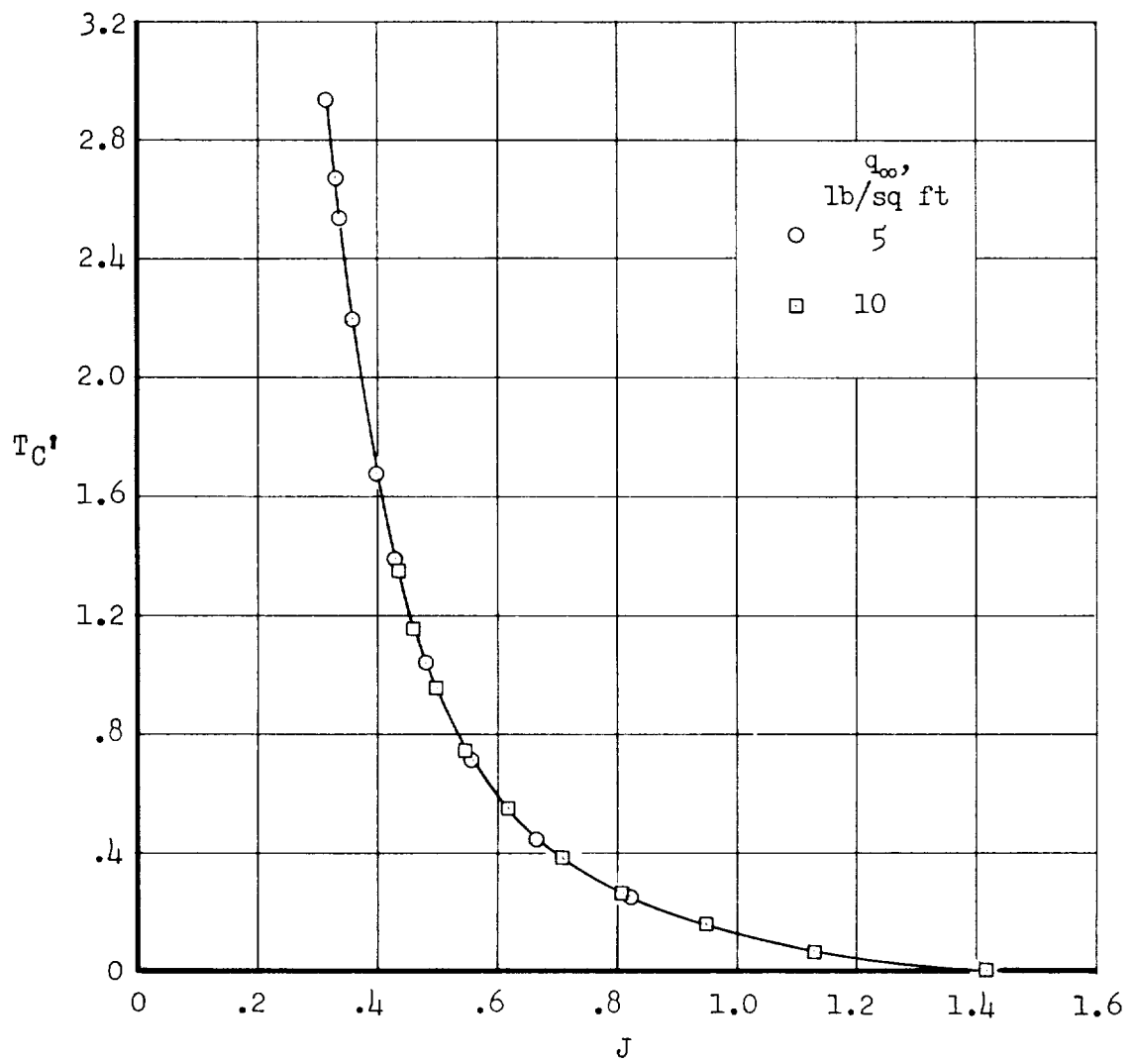
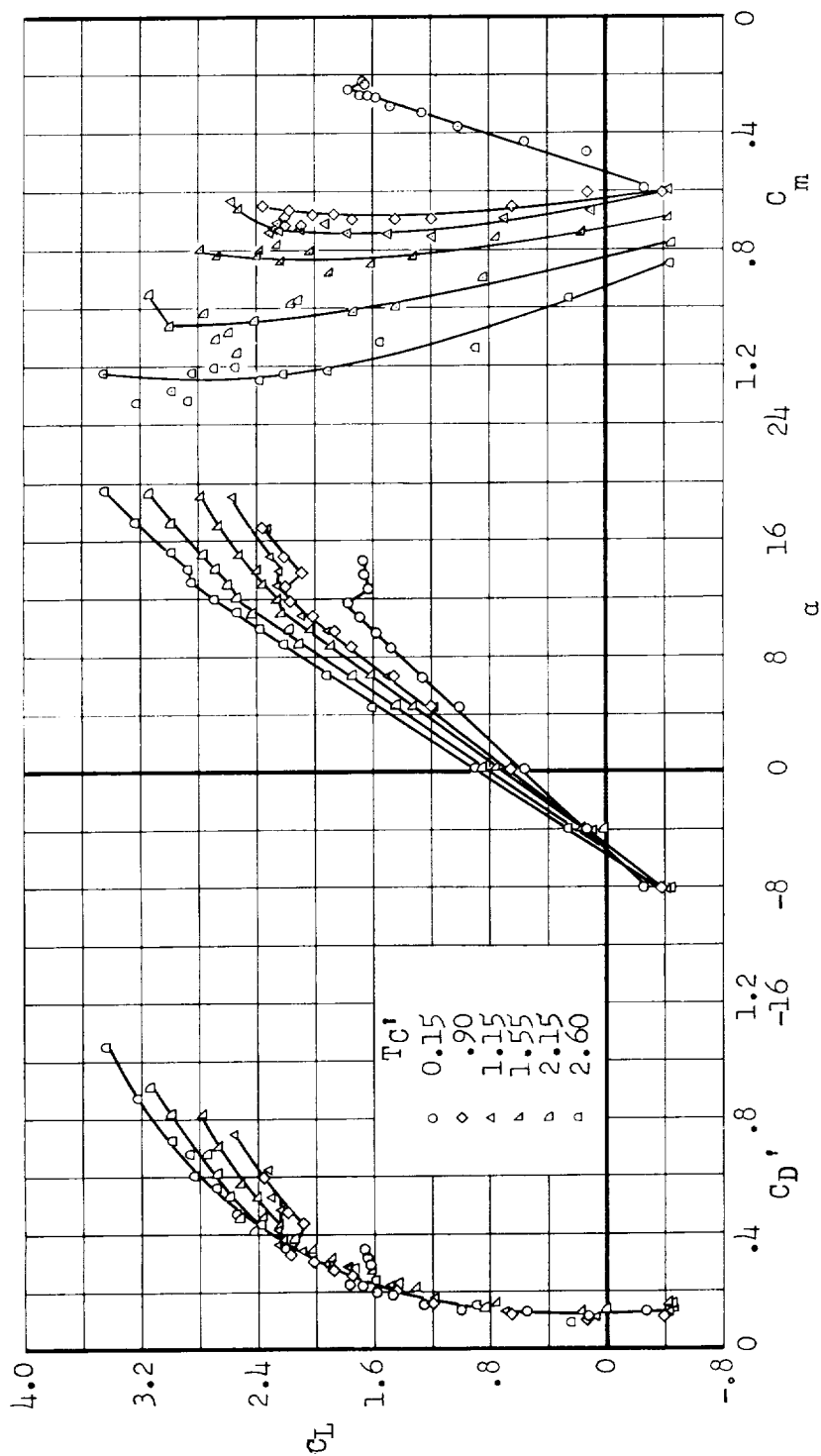
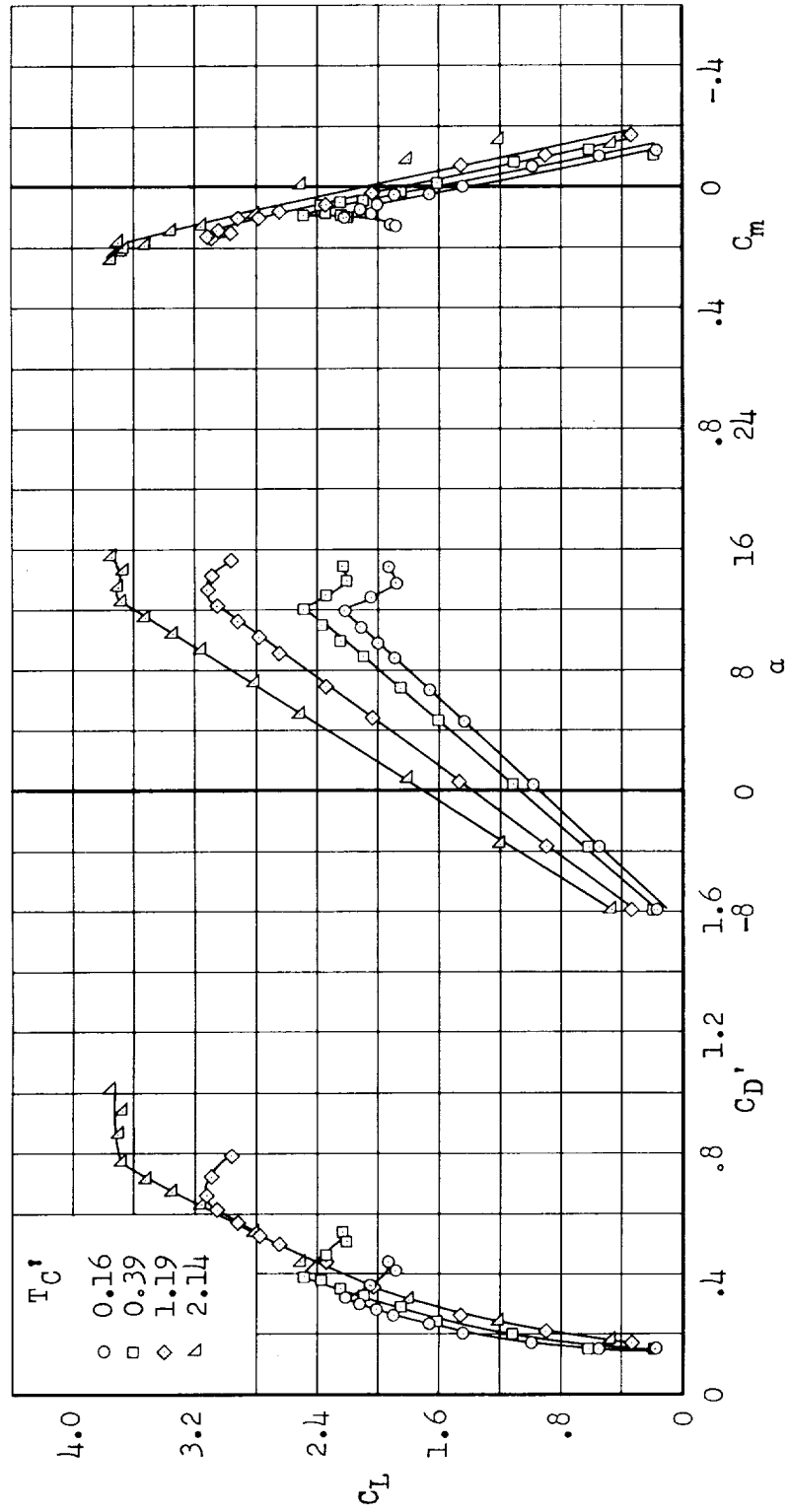


Figure 4.- Propeller thrust characteristics; two-propeller operation.



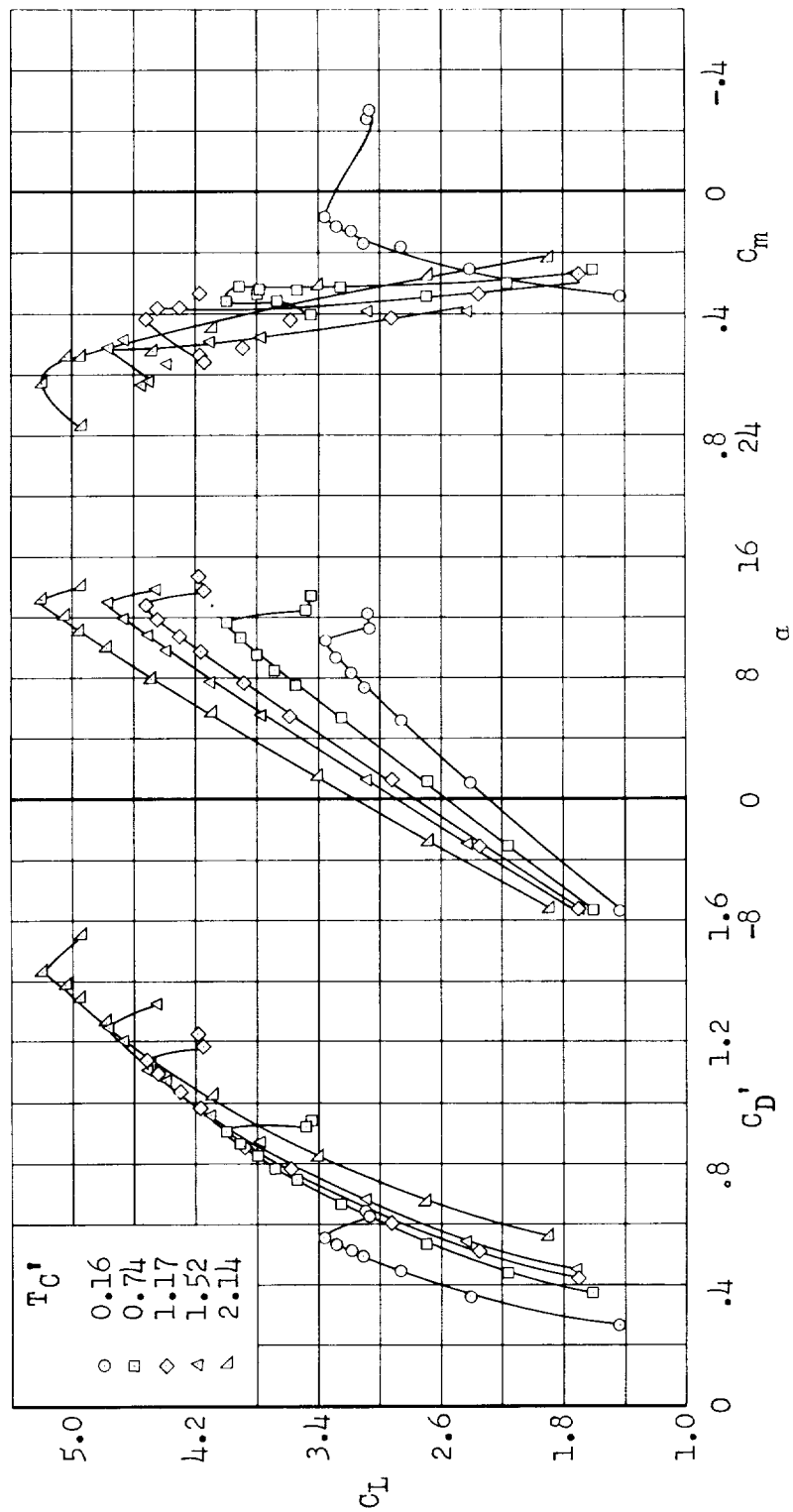
(a) $\delta_f = \delta_a = 0$; $C_{\mu f} = C_{\mu a} = 0$; $i_t = -3^\circ$

Figure 5.- Effect of thrust coefficient on the aerodynamic characteristics of the model.



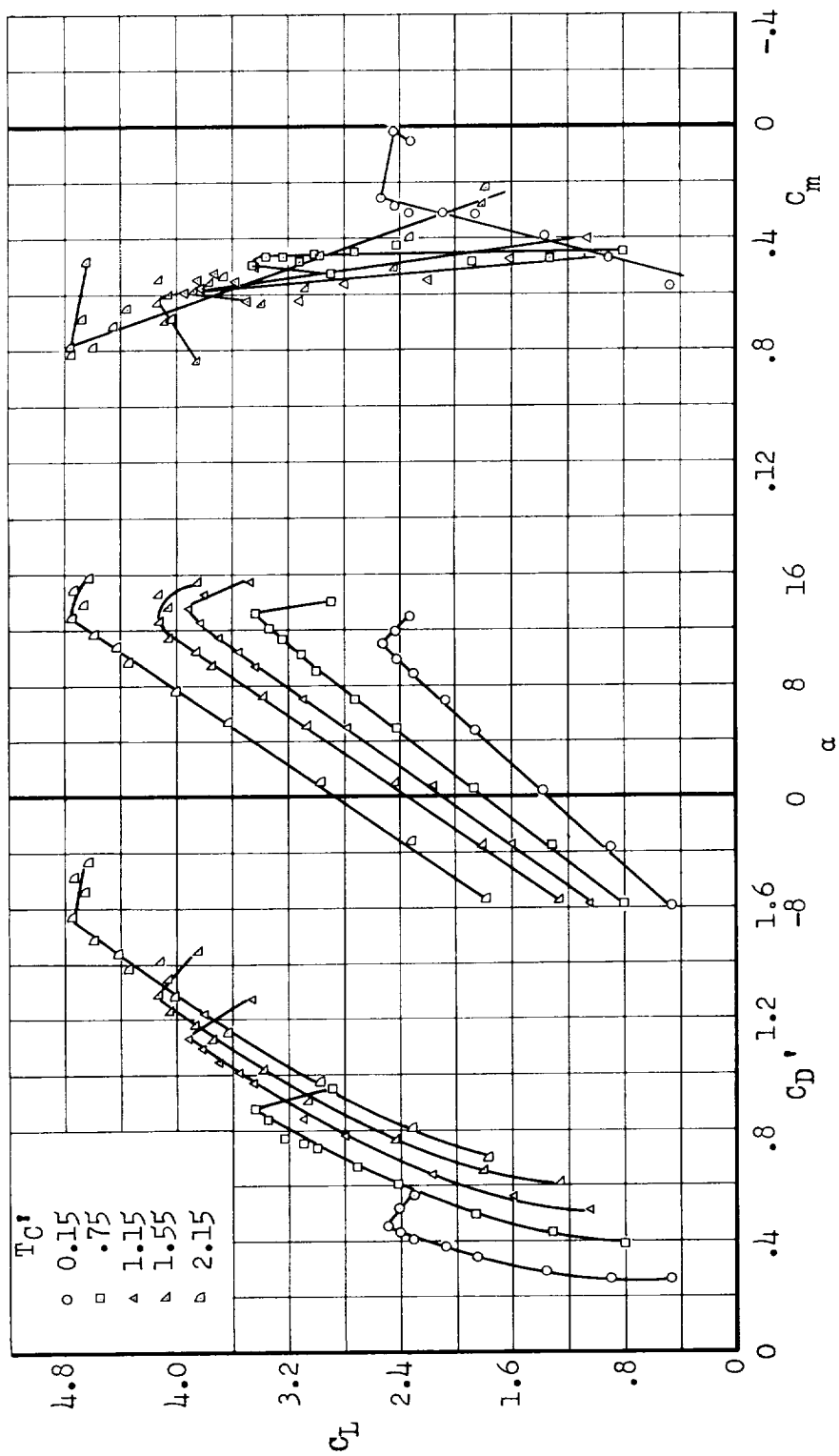
(b) $\delta_F = 20^\circ$; $\delta_a = 0^\circ$; $C_{\mu_f} = C_{\mu_a} = 0$; horizontal and vertical tails off.

Figure 5.- Continued.



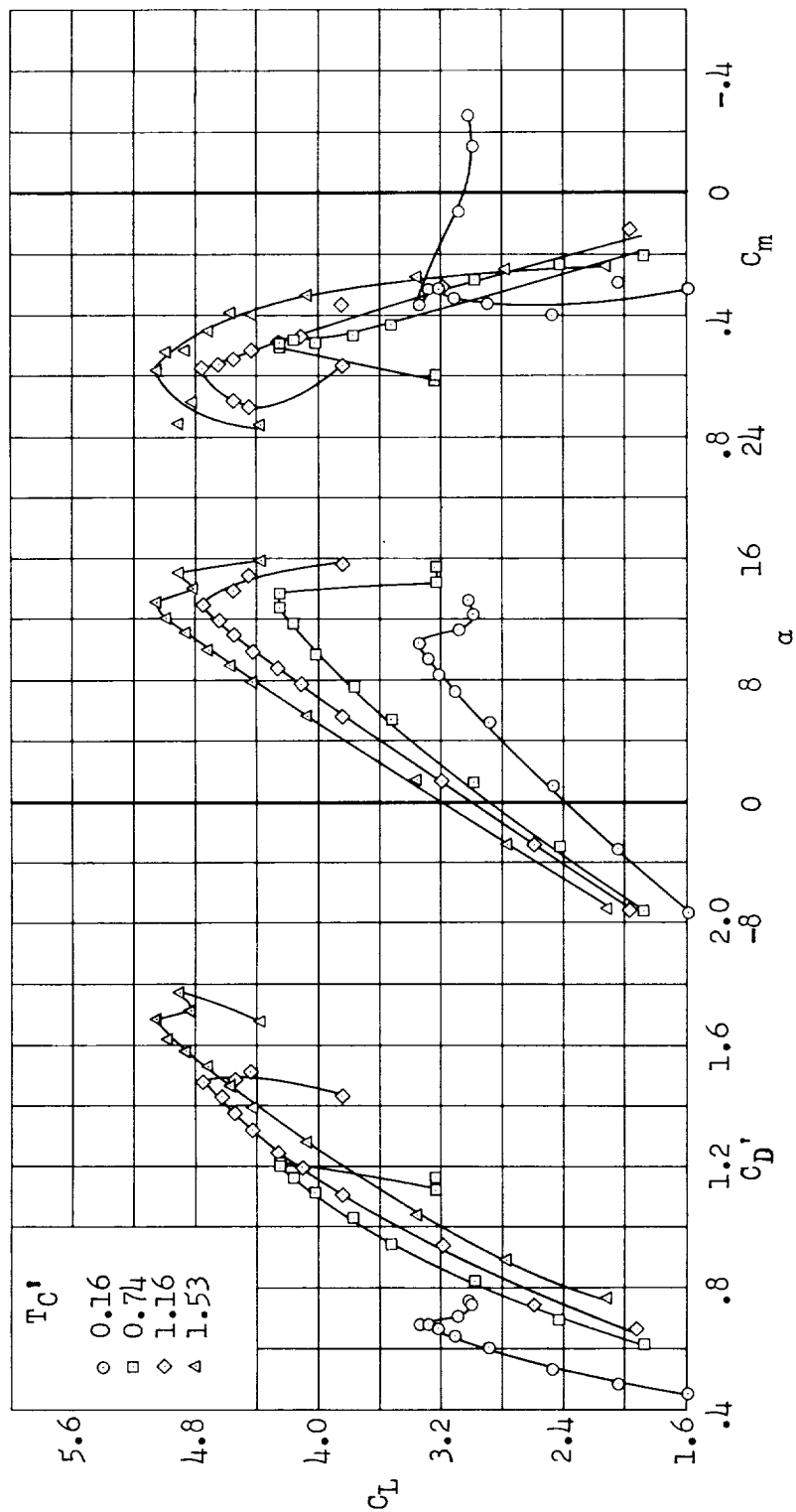
(d) $\delta_f = 40^\circ$; $\delta_a = 30^\circ$; $C_{\mu_f} = 0.030$; $C_{\mu_a} = 0.005$; $i_t = -3^\circ$

Figure 5.- Continued.



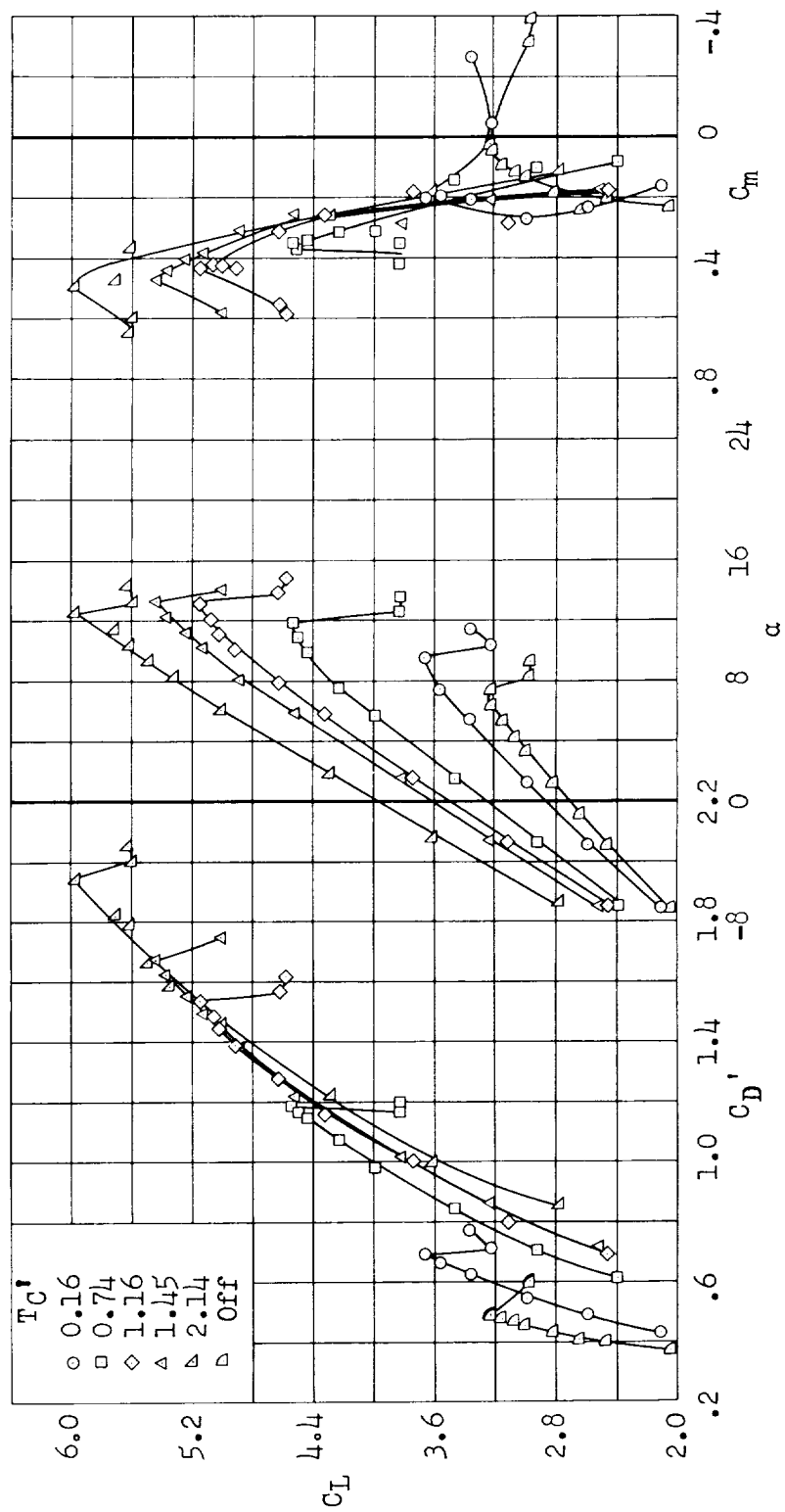
(e) $\delta_f = 60^\circ$; $\delta_a = 0^\circ$; $C_{\mu_f} = C_{\mu_a} = 0$; $i_t = -3^\circ$

Figure 5.- Continued.



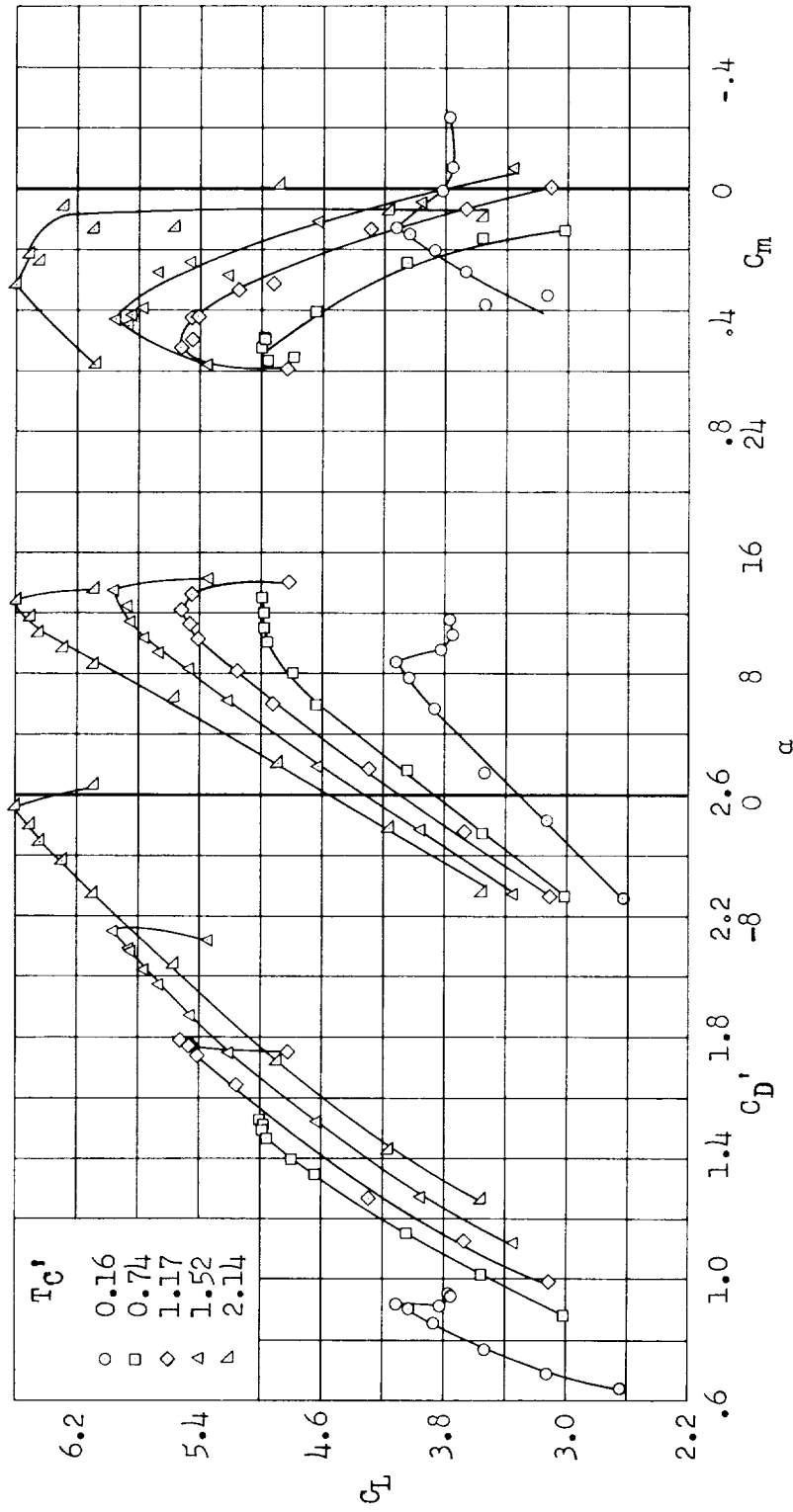
(f) $\delta_f = 60^\circ$; $\delta_a = 0^\circ$; $C_{\mu_f} = 0.035$; $C_{\mu_a} = 0$; $i_t = -3^\circ$

Figure 5.- Continued.



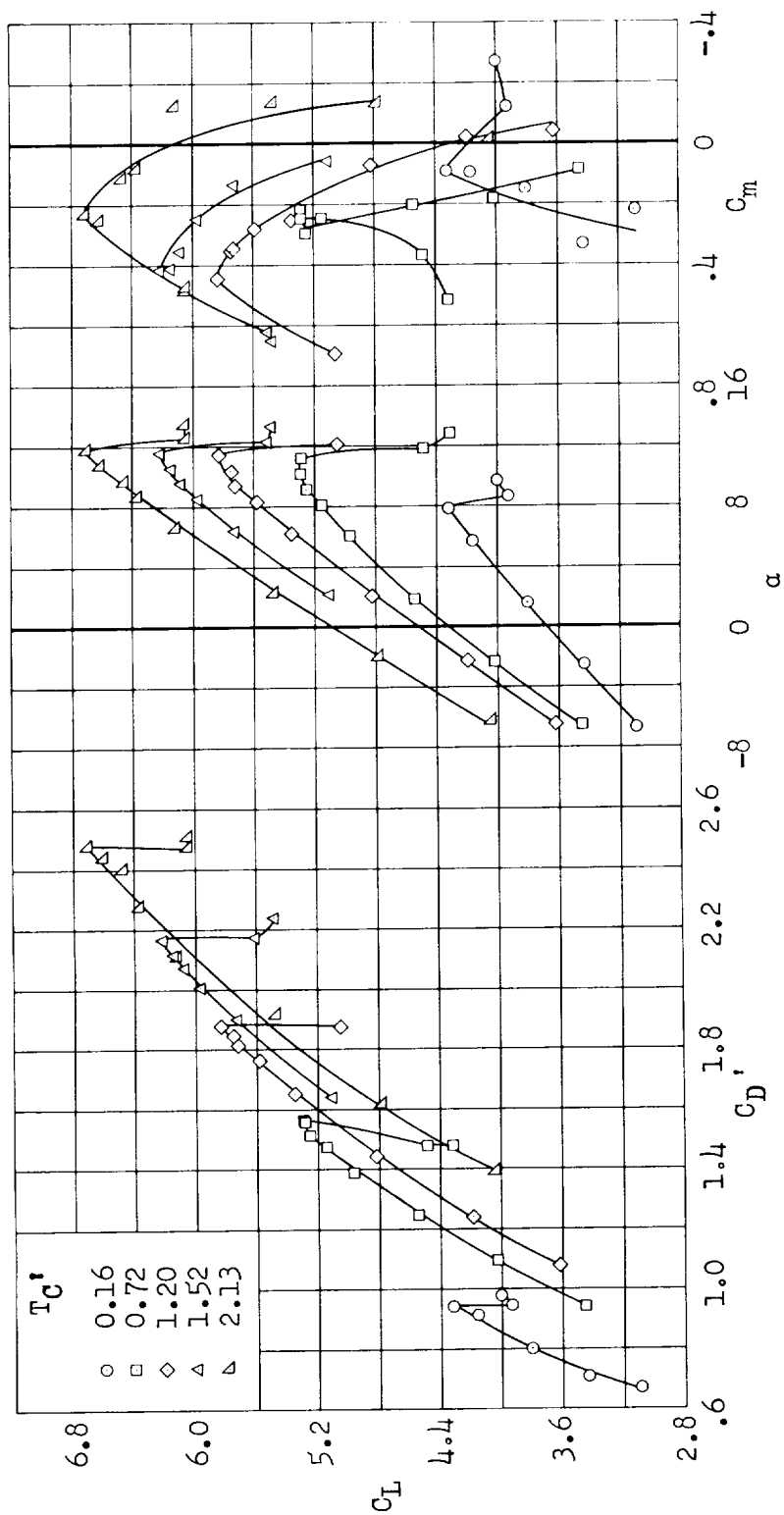
(g) $\delta_f = 60^\circ$; $\delta_a = 30^\circ$; $C_{\mu_f} = 0.035$; $C_{\mu_a} = 0.004$; $i_t = -3^\circ$

Figure 5.- Continued.



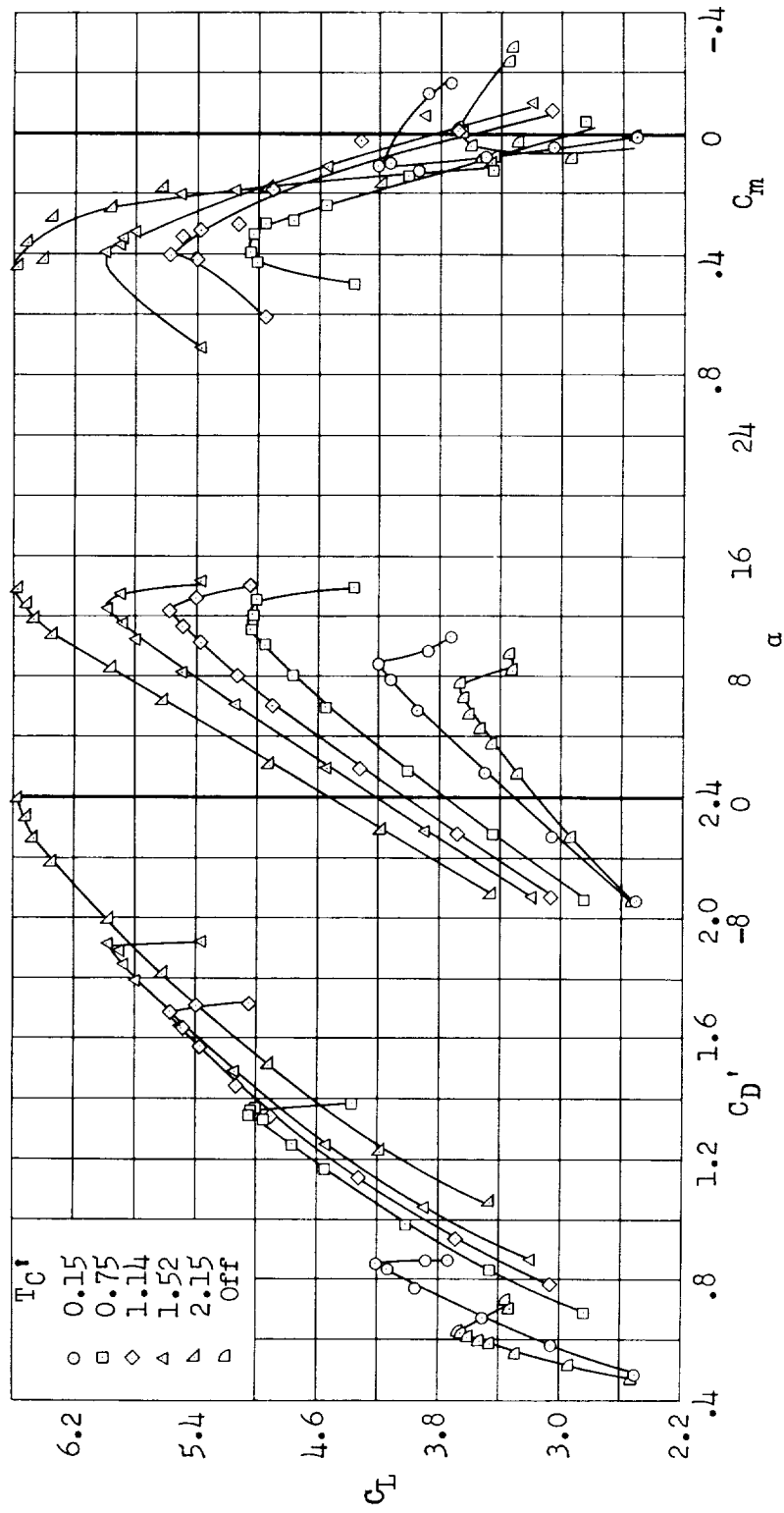
(h) $\delta_f = 80^\circ$; $\delta_a = 30^\circ$; $C_{\mu_f} = 0.057$; $C_{\mu_a} = 0.005$; $i_t = -3^\circ$

Figure 5.- Continued.



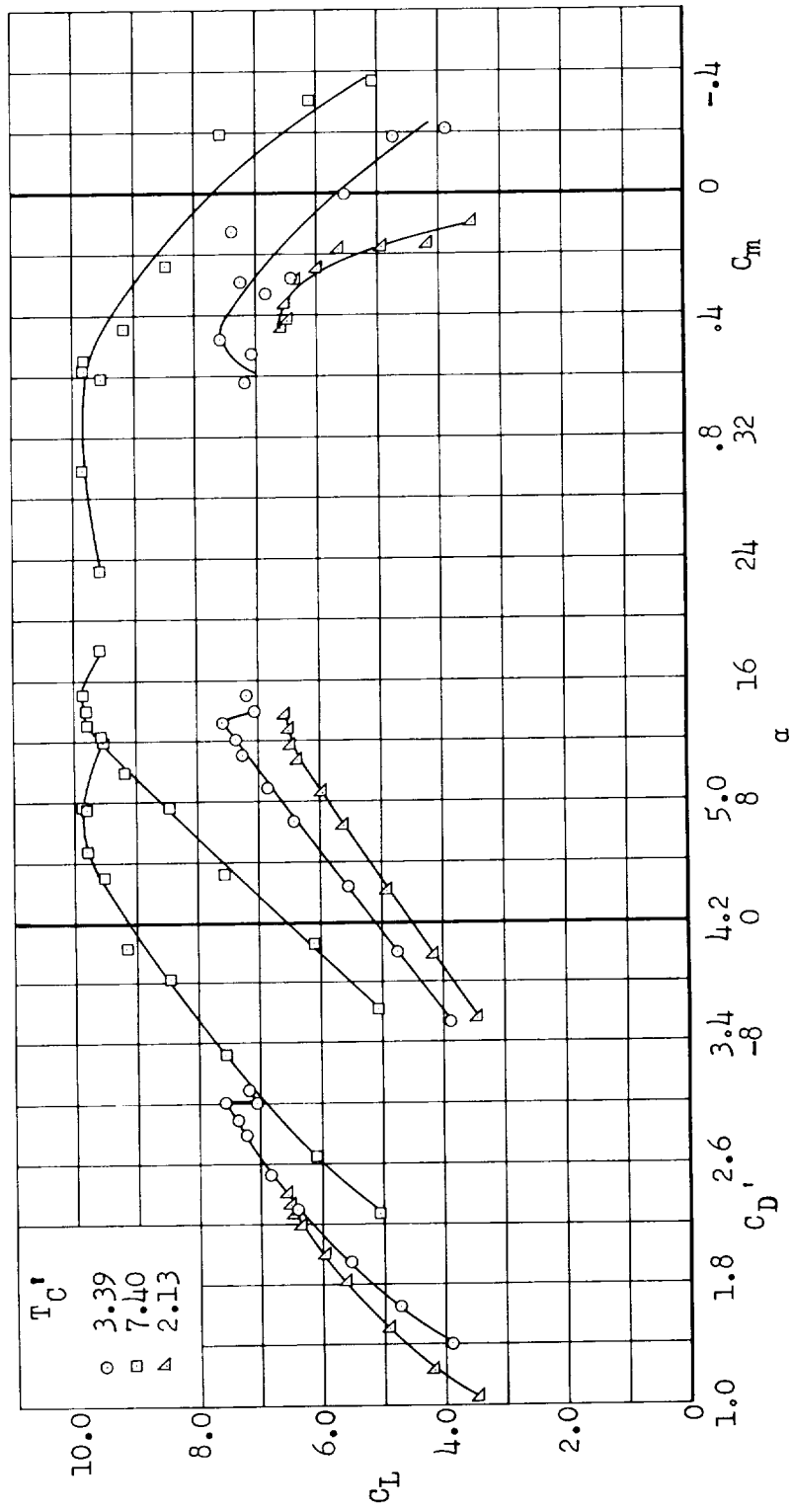
(i) $\delta_F = 80^\circ$; $\delta_a = 50^\circ$; $C_{\mu_f} = 0.059$; $C_{\mu_a} = 0.027$

Figure 5.- Concluded.



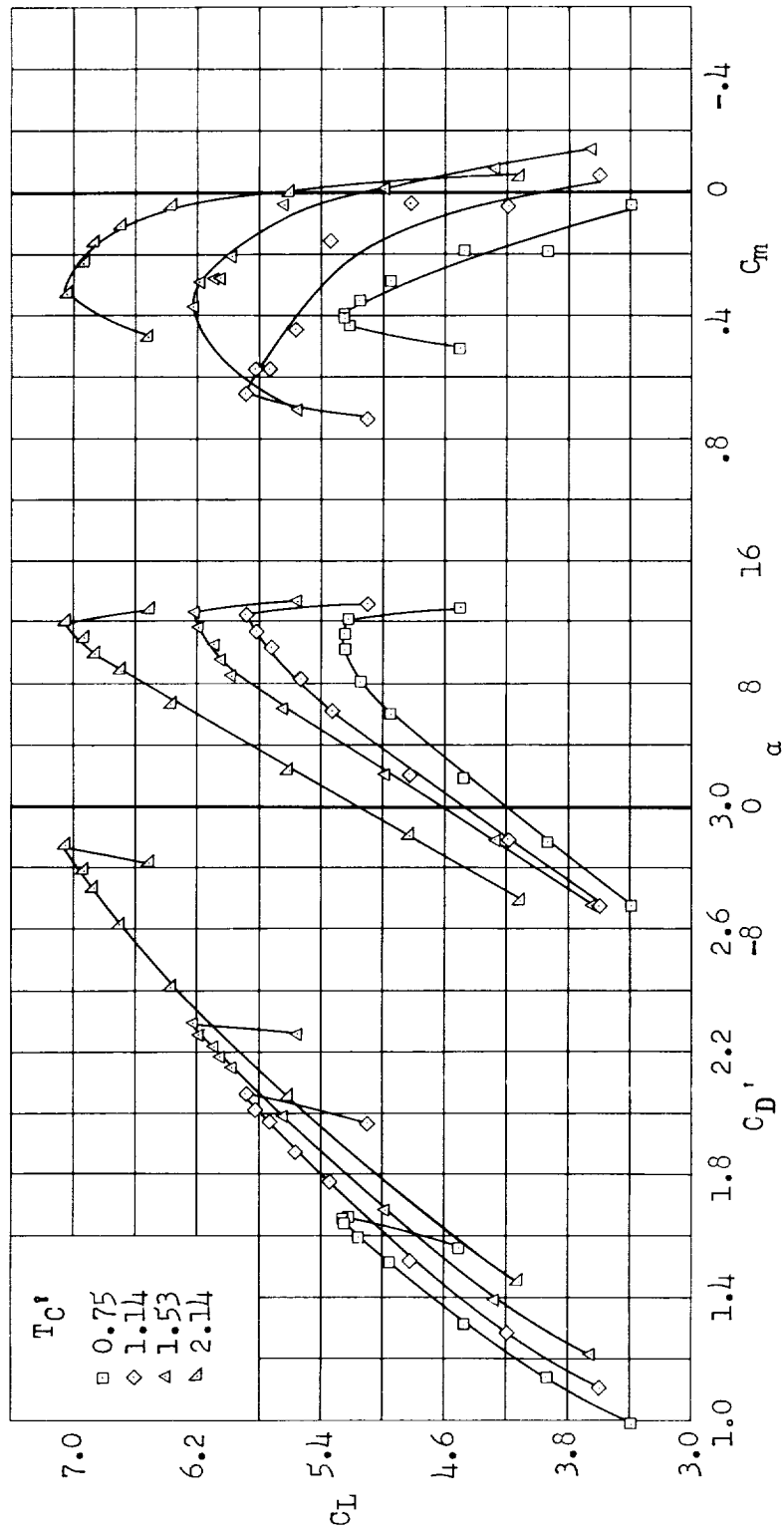
(a) $\delta_f = 60^\circ$; $\delta_a = 30^\circ$; $C_{\mu_f} = 0.097$; $C_{\mu_a} = 0.008$; $i_t = -3^\circ$

Figure 6.- Effect of thrust coefficient on the aerodynamic characteristics of the model.



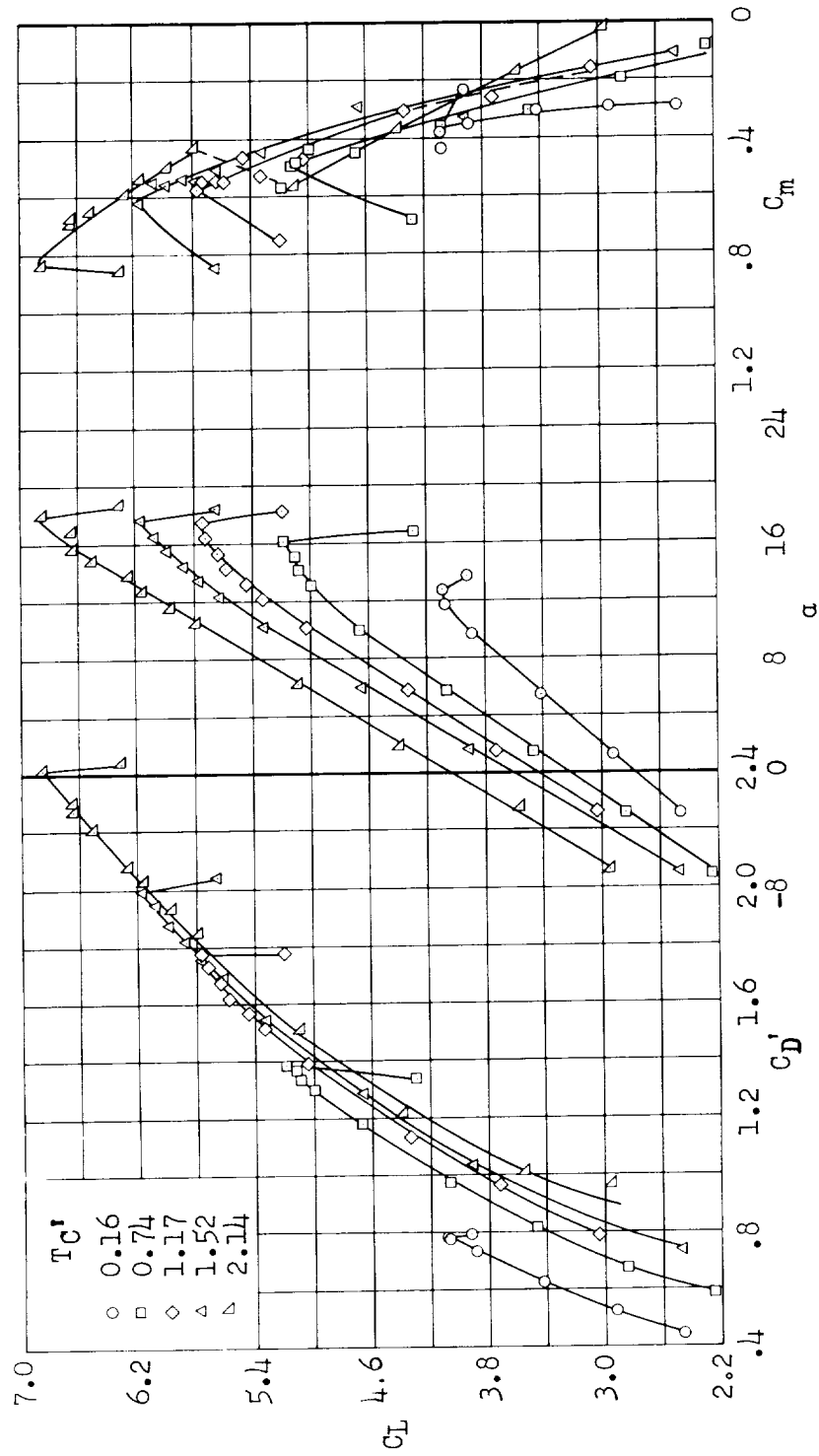
(b) $\delta_F = 60^\circ$; $\delta_a = 30^\circ$; $C_{\mu_F} = 0.097$; $C_{\mu_a} = 0.008$; $i_t = -3^\circ$

Figure 6.- Continued.



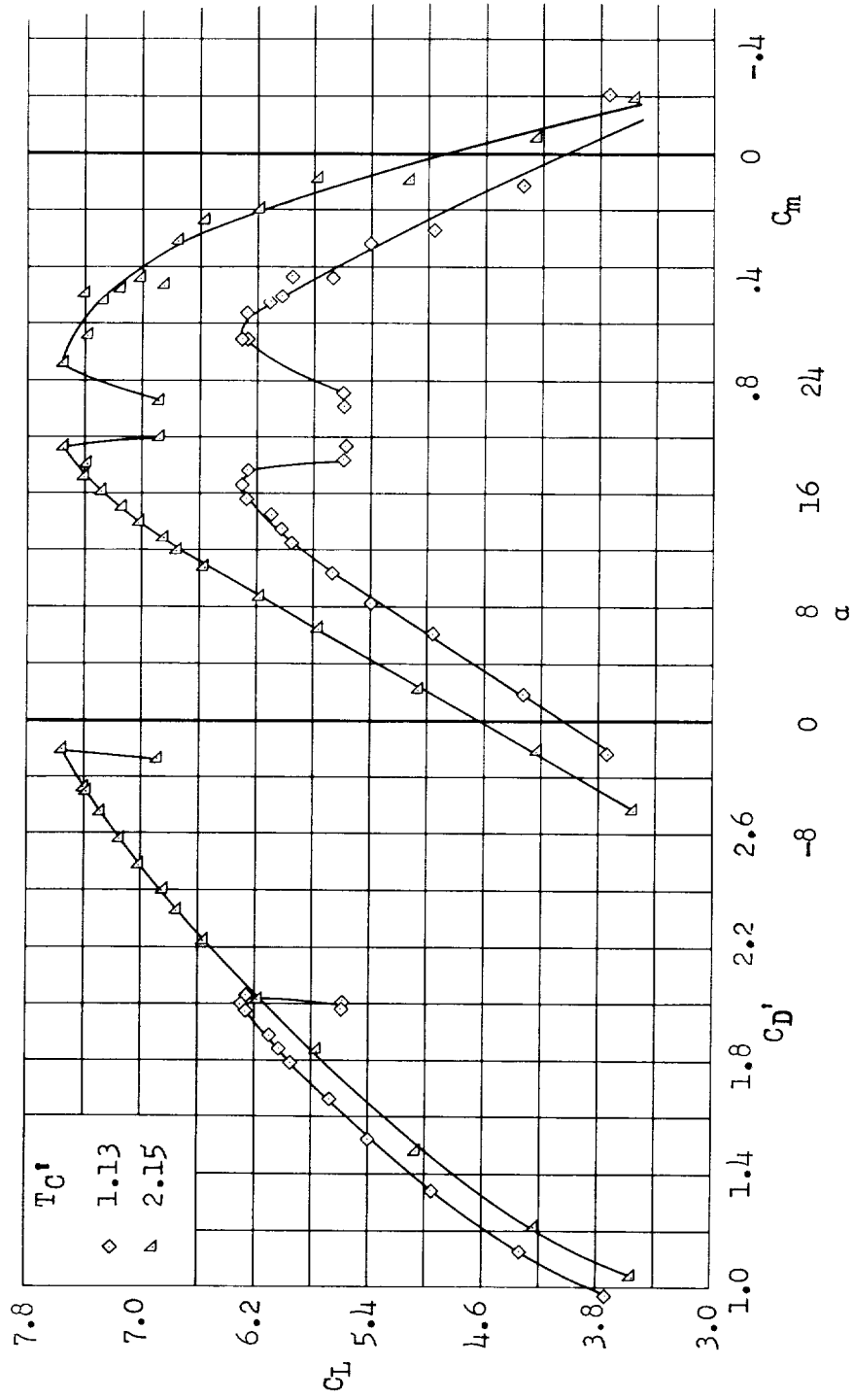
(c) $\delta_f = 80^\circ$; $\delta_a = 30^\circ$; $C_{\mu_f} = 0.095$; $C_{\mu_a} = 0.008$; $i_t = -3^\circ$

Figure 6.- Concluded.



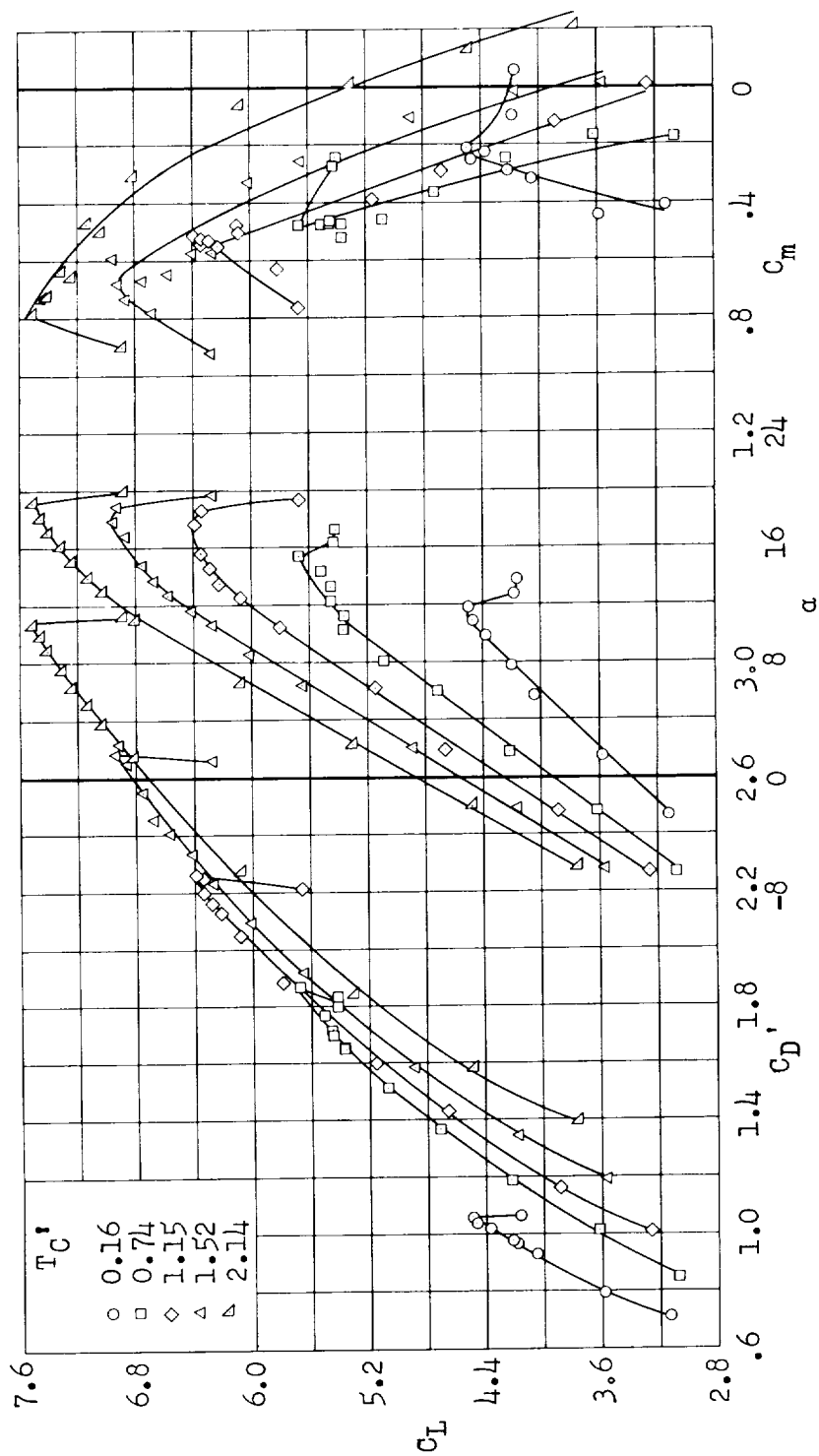
(a) $\delta_f = 60^\circ$; $\delta_a = 30^\circ$; $C_{\mu_f} = 0.034$; $C_{\mu_a} = 0.004$; $i_t = -3^\circ$

Figure 7.- Aerodynamic characteristics of the model with a simulated leading-edge flap.



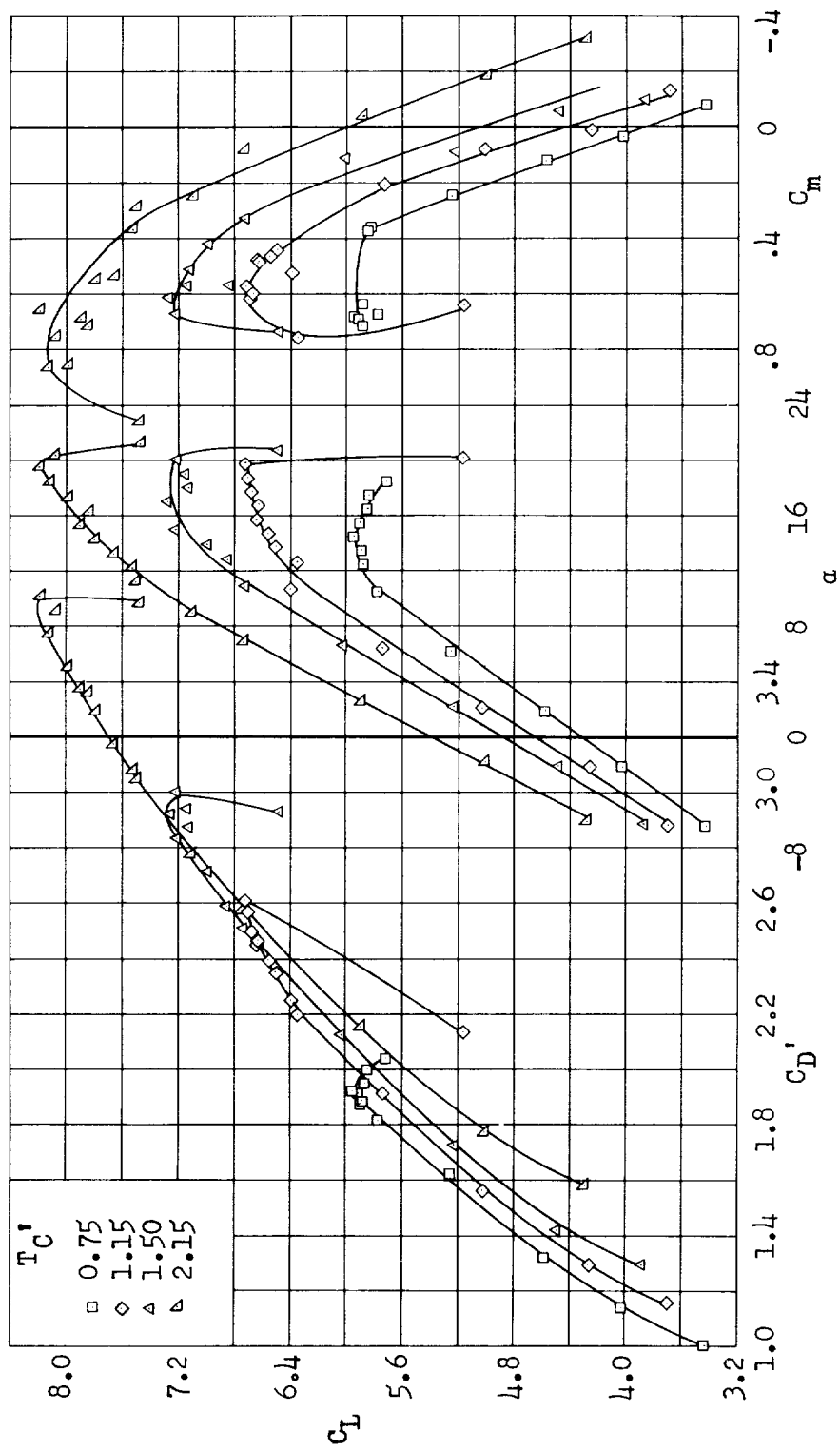
(b) $\delta_f = 60^\circ$; $\delta_a = 30^\circ$; $C_{\mu_f} = 0.096$; $C_{\mu_a} = 0.008$; $i_t = -3^\circ$

Figure 7.- Continued.



(c) $\delta_f = 80^\circ$; $\delta_a = 30^\circ$; $C_{\mu_f} = 0.056$; $C_{\mu_a} = 0.005$; $i_t = -3^\circ$

Figure 7.- Continued.



(d) $\delta_f = 80^\circ$; $\delta_a = 30^\circ$; $C_{\mu_f} = 0.097$; $C_{\mu_a} = 0.008$; $i_t = -3^\circ$

Figure 7.- Concluded.

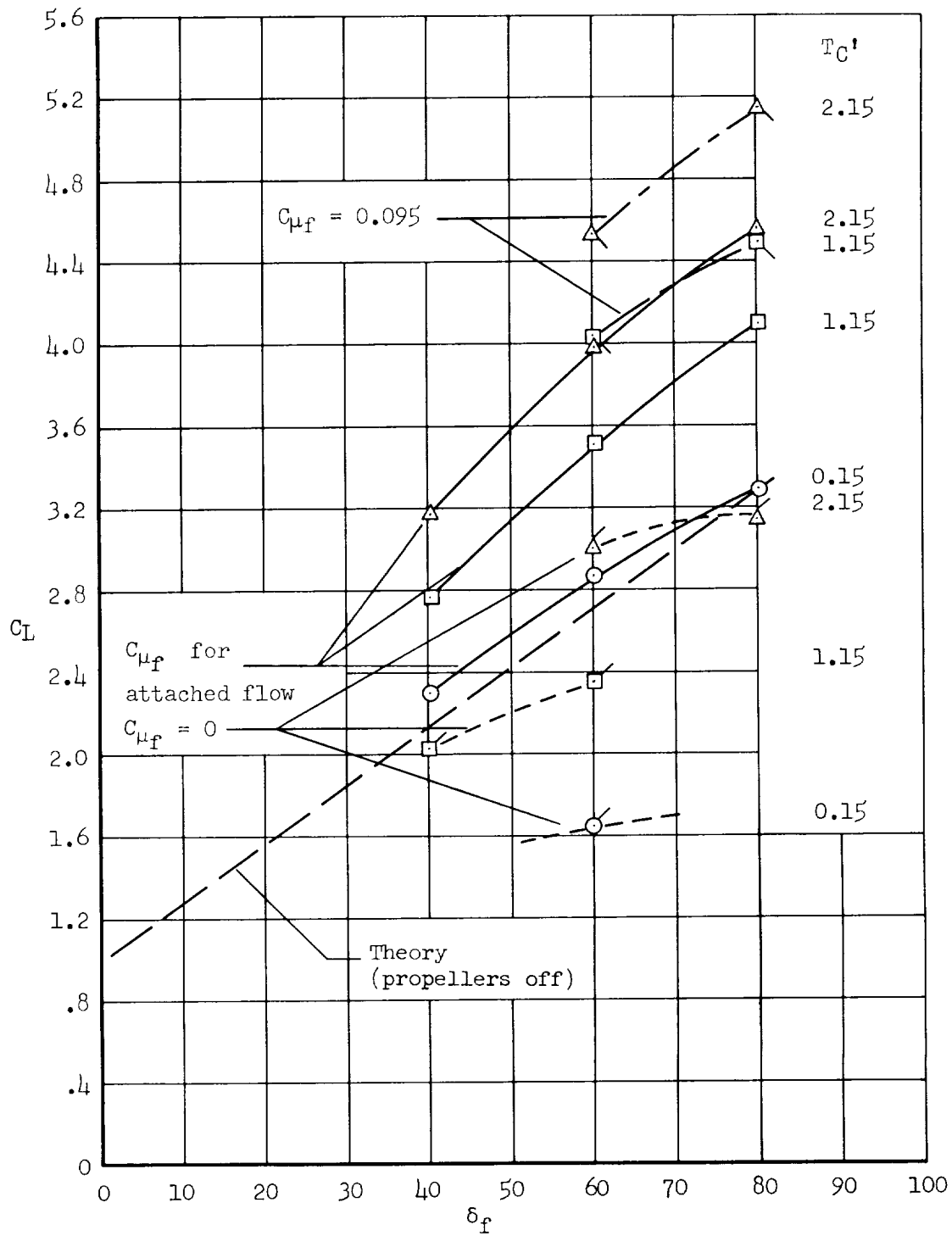


Figure 8.- Effect of thrust coefficient and flap-momentum coefficient on the variation of lift with flap deflection at 0° angle of attack; $\delta_a = 30^\circ$, $C_{\mu a} = 0.003$, $i_t = -3^\circ$.

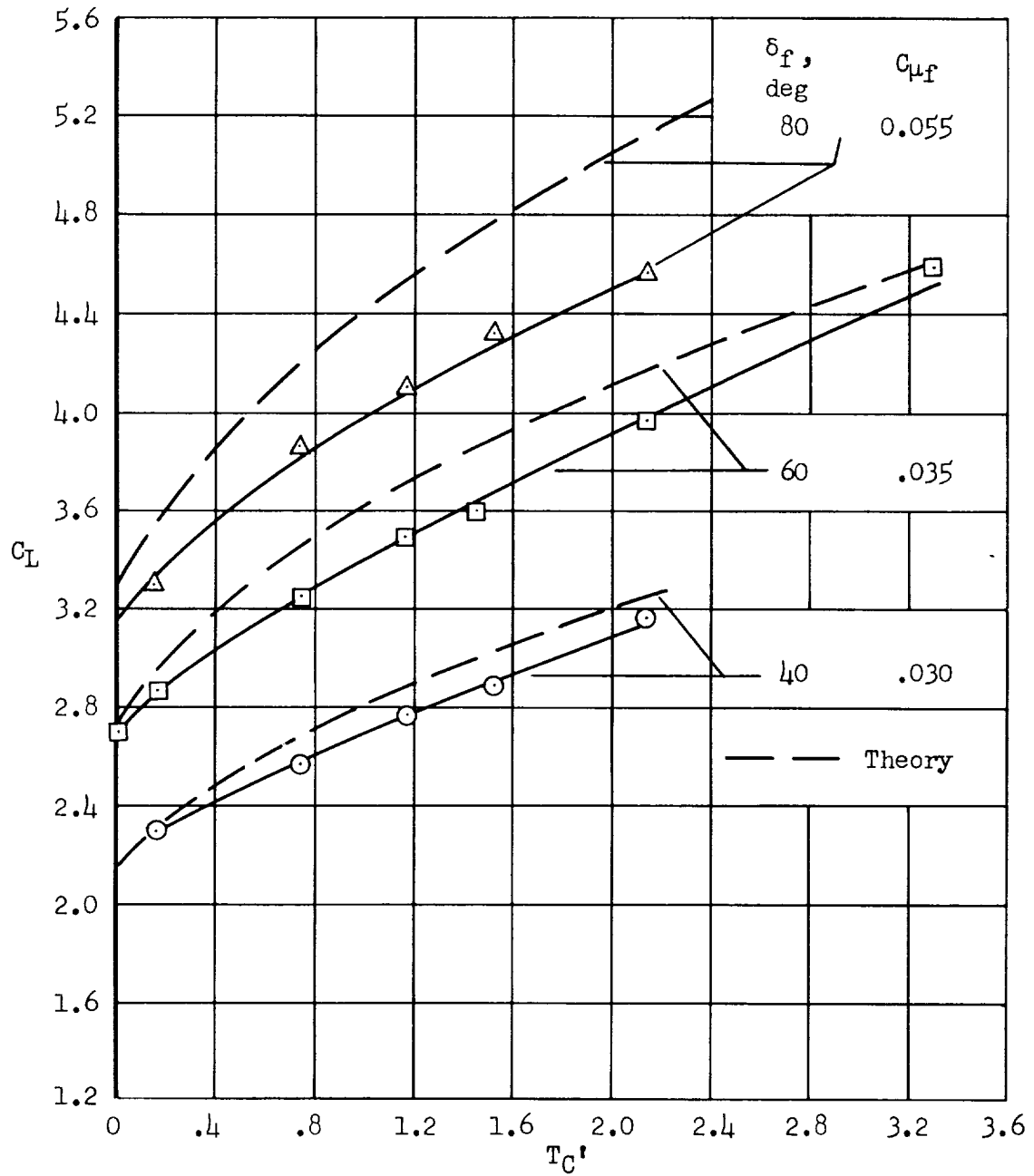


Figure 9.- The effect of thrust coefficient on the lift coefficient at 0° angle of attack; $\delta_a = 30^\circ$, $C_{\mu_a} = 0.003$.

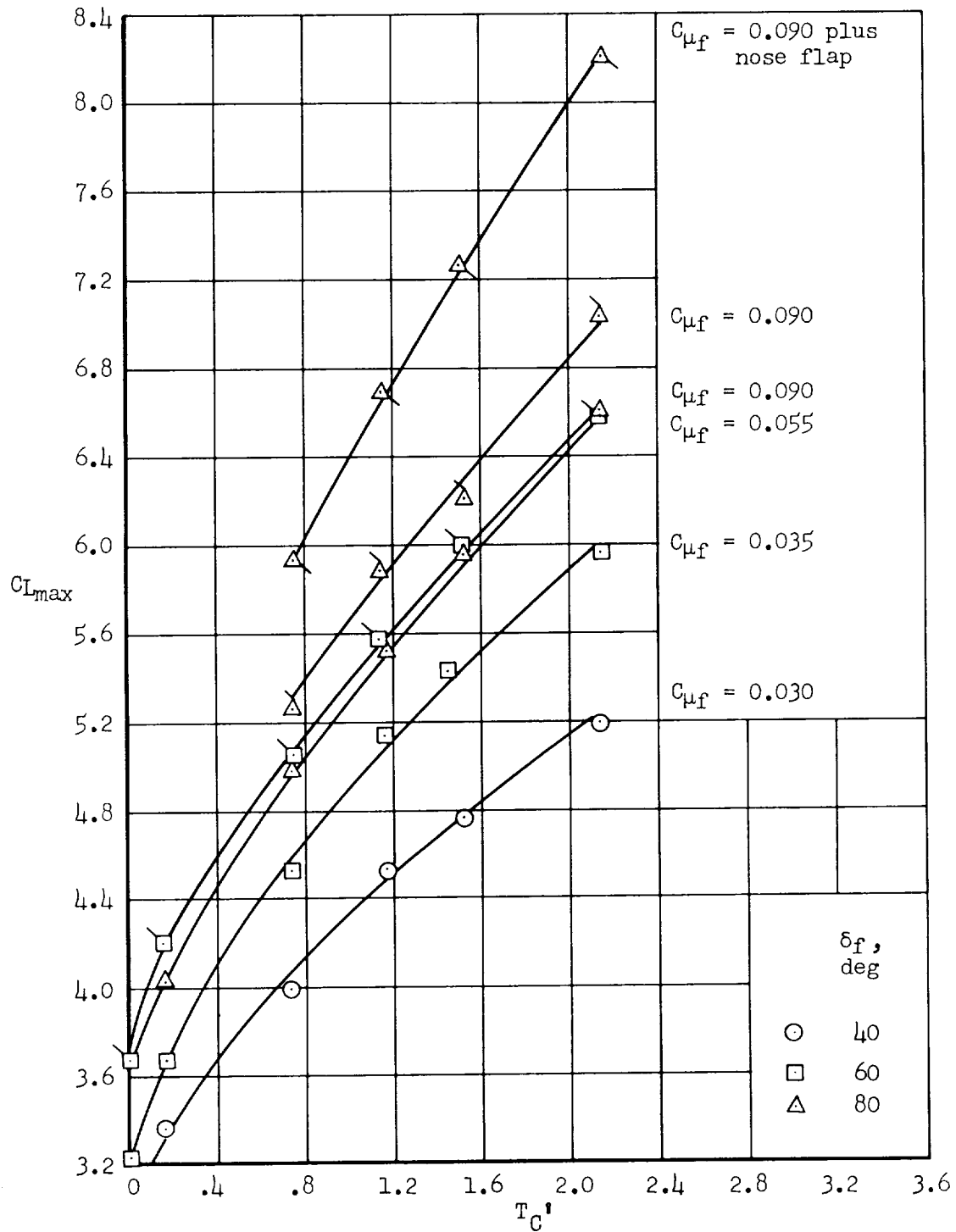
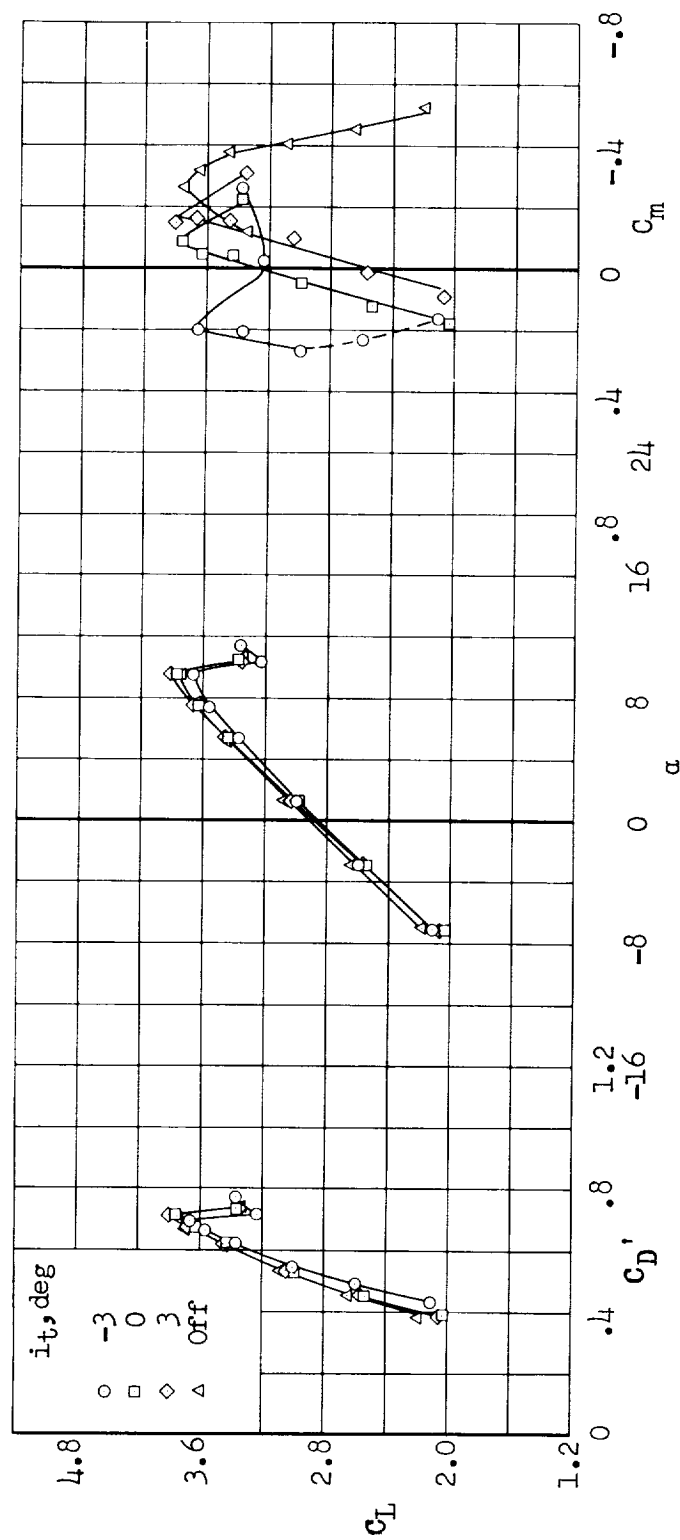
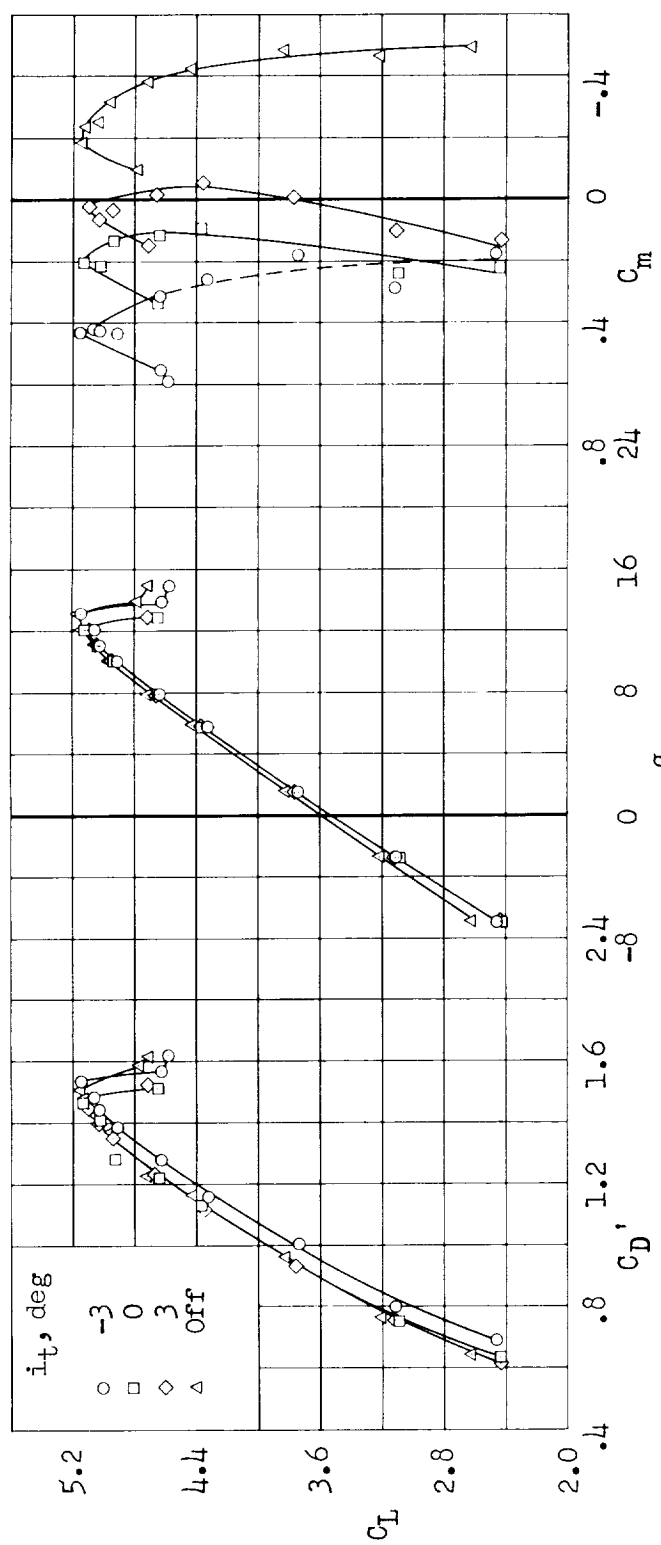


Figure 10.- The effects of flap deflection, flap momentum coefficient, and simulated nose flap on the variation of $C_{L_{max}}$ with thrust coefficient; $\delta_a = 30^\circ$, $C_{\mu_a} = 0.003$.



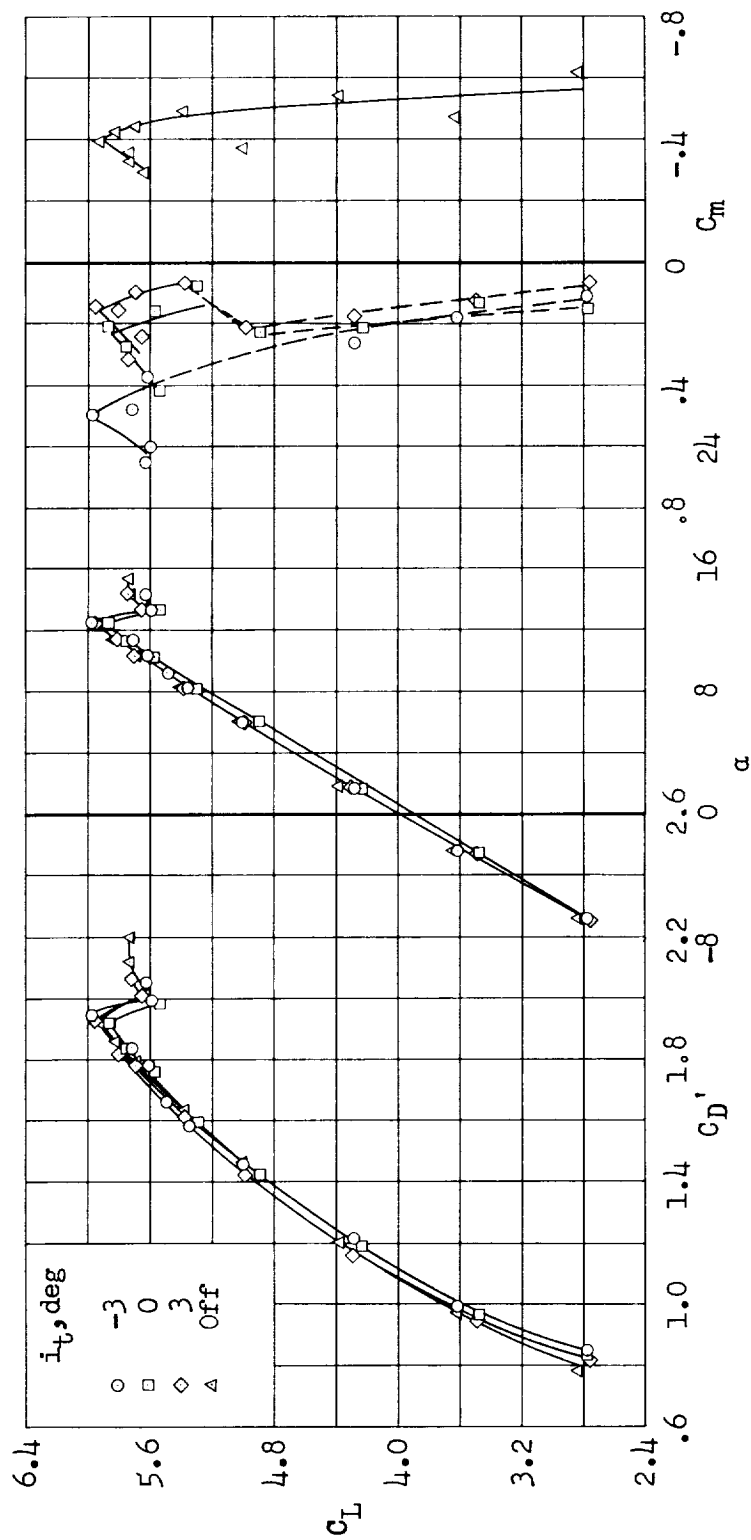
(a) $T_C' = 0.16$

Figure 11.- Effect of horizontal tail on aerodynamic characteristics of model; $\delta_f = 60^\circ$, $\delta_a = 30^\circ$, $C_{\mu_f} = 0.035$, $C_{\mu_a} = 0.004$.



(b) $T_C' = 1.14$

Figure 11.- Continued.



(c) $T_C' = 2.14$

Figure 11.- Concluded.

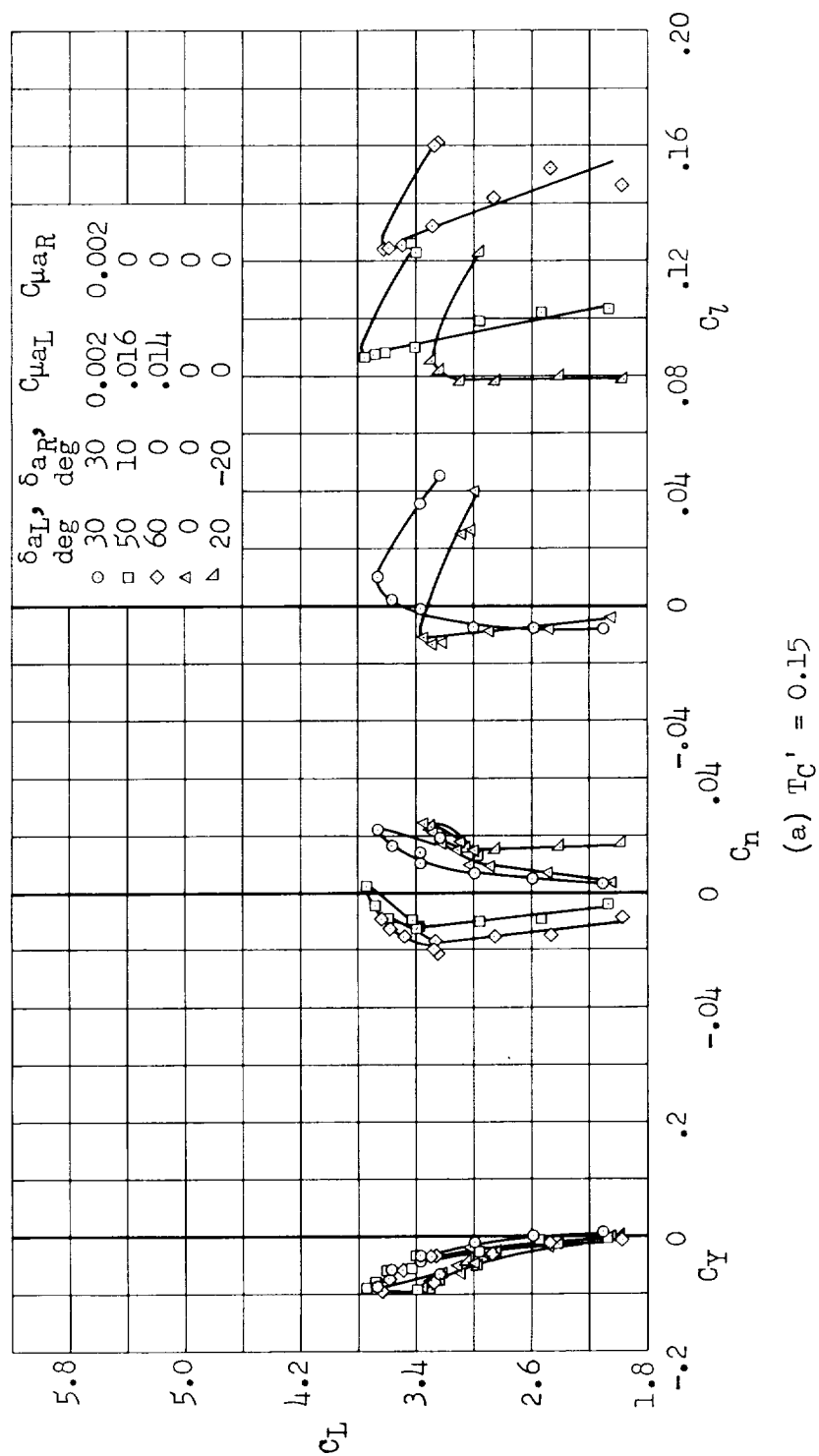
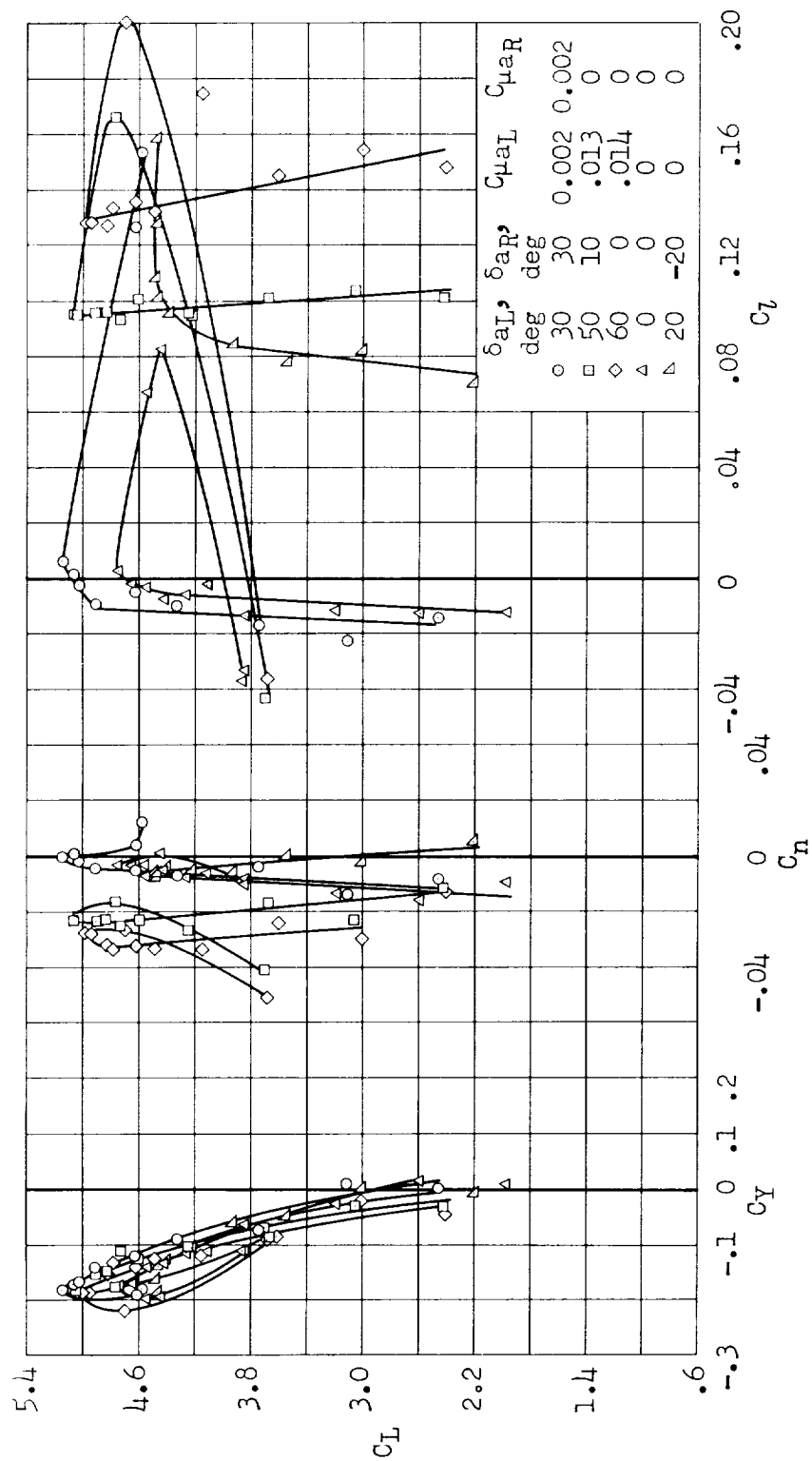
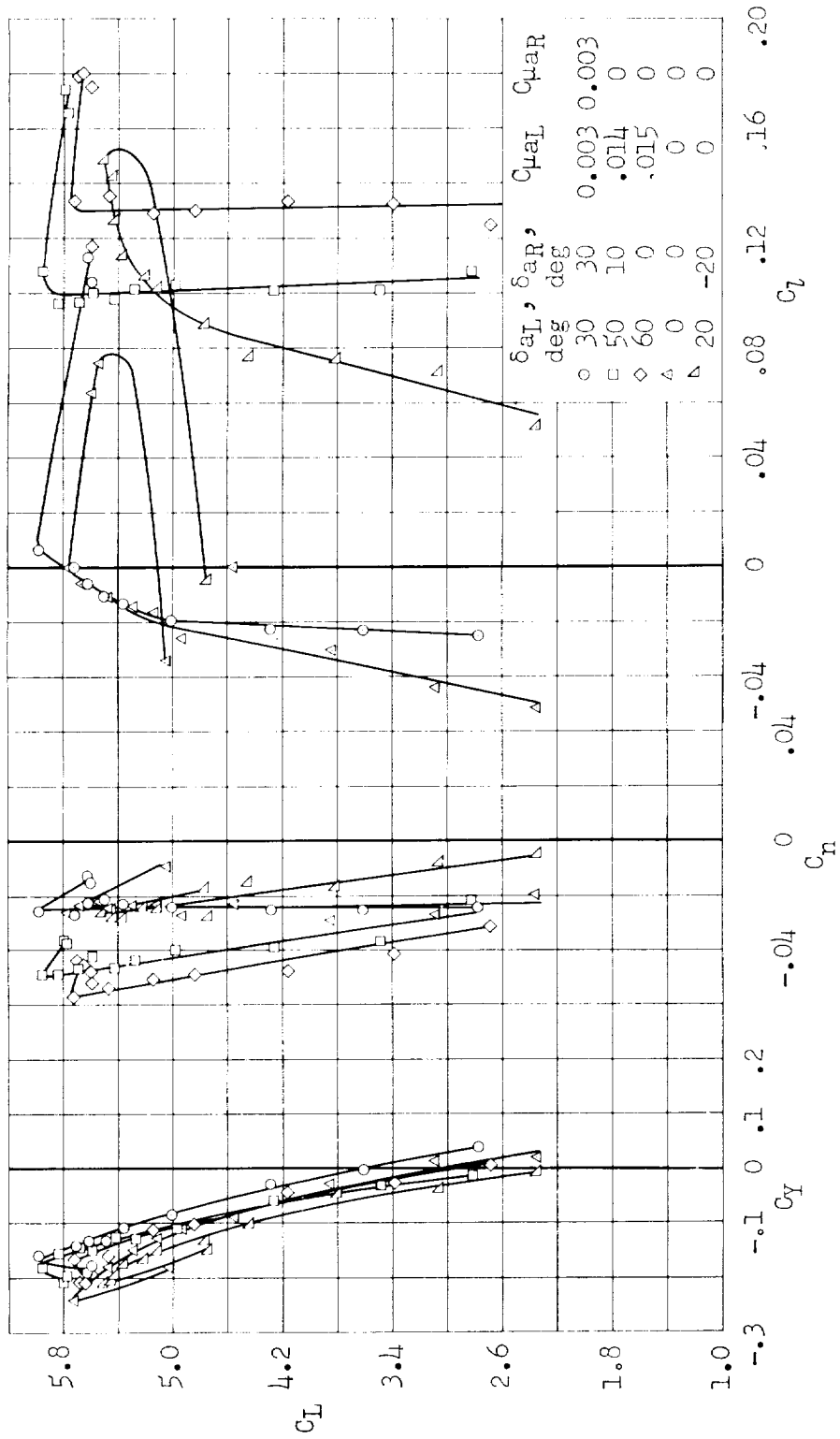


Figure 12.- Effect of aileron deflection on side-force, yawing-moment, and rolling-moment coefficients; $\delta_a = 60^\circ$, $C_{\mu F} = 0.035$, $i_t = -3^\circ$.



(b) $T_C' = 1.15$

Figure 12.- Continued.



(c) $T_C' = 2.15$

Figure 12.- Concluded.

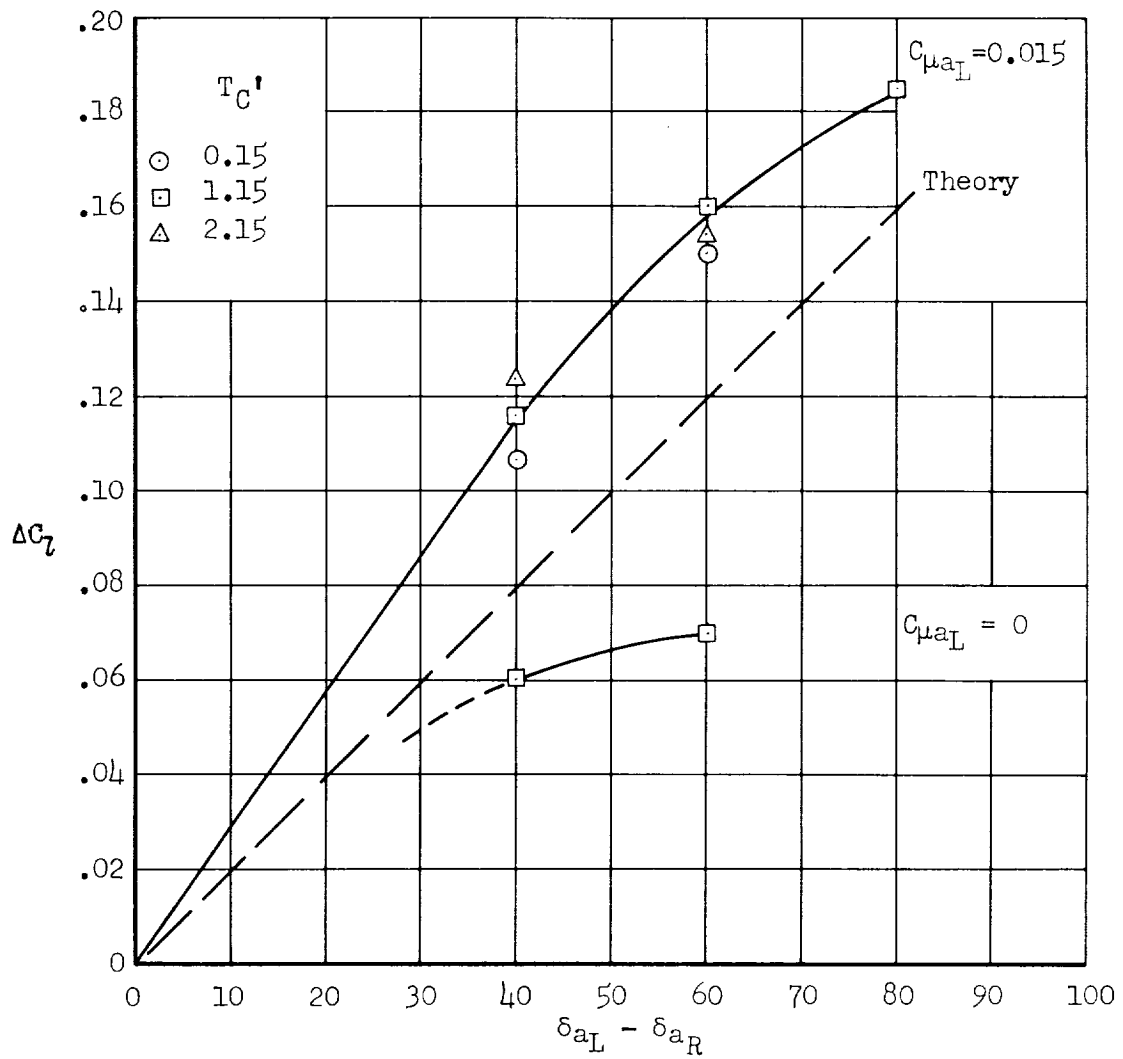


Figure 13.- Comparison with theory (ref. 5) of rolling moment produced by deflection of ailerons differentially about a 30° aileron droop; $\delta_f = 60^\circ$, $C_{\mu_f} = 0.035$, $\alpha_u = 0^\circ$.

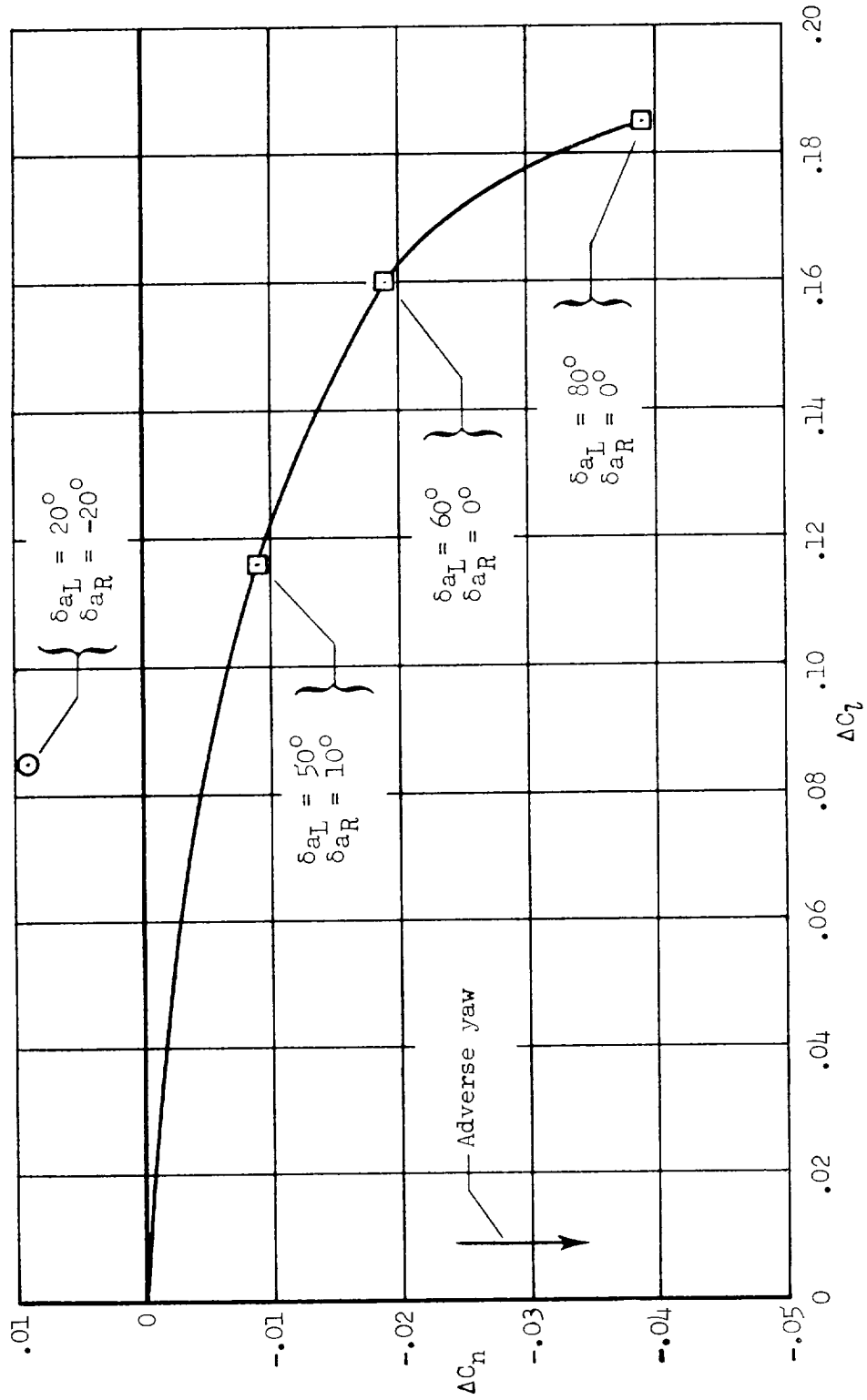
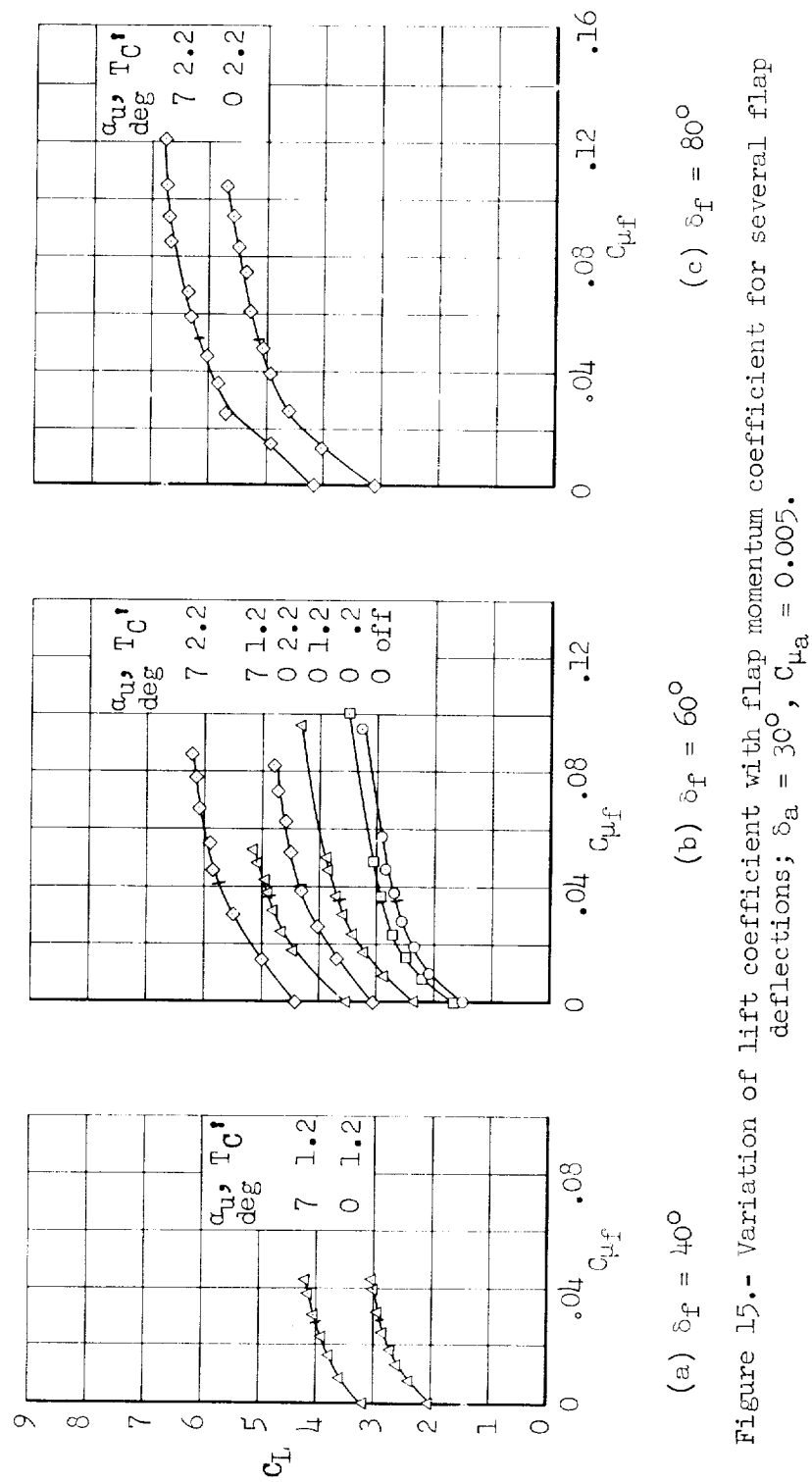


Figure 14.- Effect of differentially deflected ailerons on incremental yawing moment; $C_L = 3.4$, $T_C' = 1.15$, boundary layer control on, $\delta a_L = 50^\circ$, 60° , and 80° .



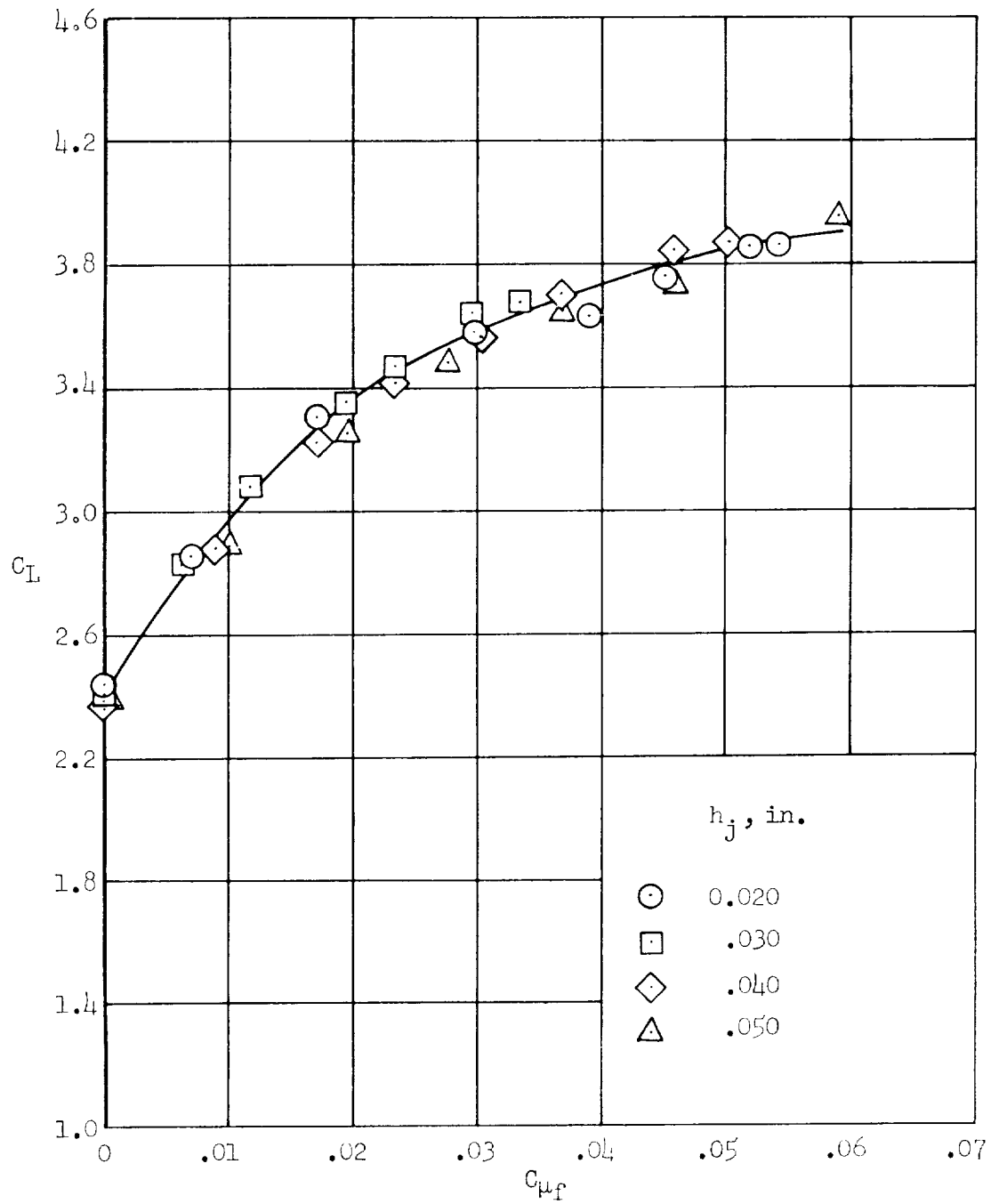


Figure 16.- Variation of C_L with C_{μ_f} for four flap nozzle heights;
 $\alpha_u = 0^\circ$, $T_C' = 1.15$, $\delta_f = 60^\circ$, $\delta_a = 30^\circ$, $C_{\mu_a} = 0.004$.

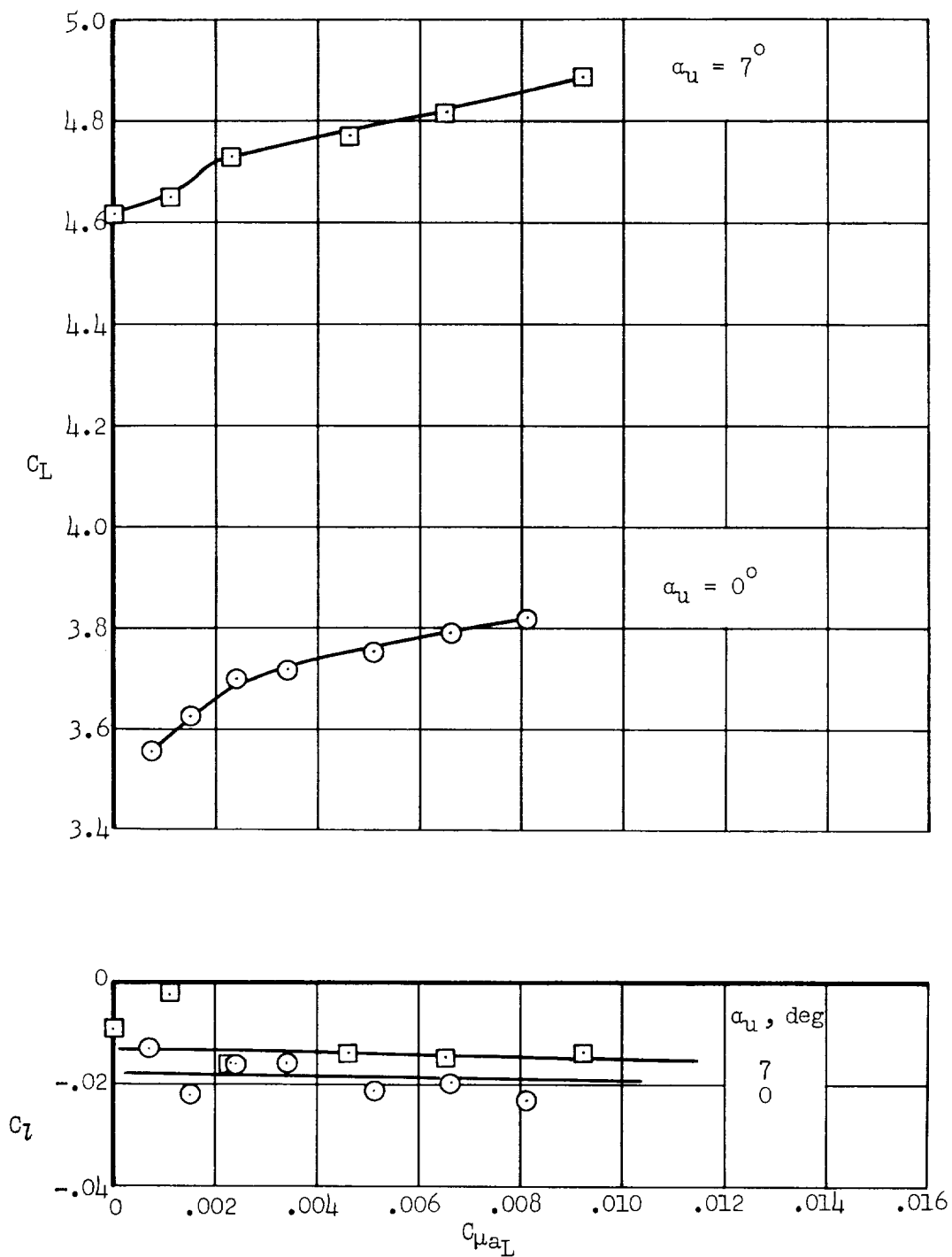


Figure 17.- Variation of lift coefficient and rolling-moment coefficient with aileron jet momentum coefficient; $\delta_{a_L} = \delta_{a_R} = 30^\circ$, $\delta_f = 60^\circ$, $C_{\mu_f} = 0.035$, $T_C' = 1.15$.

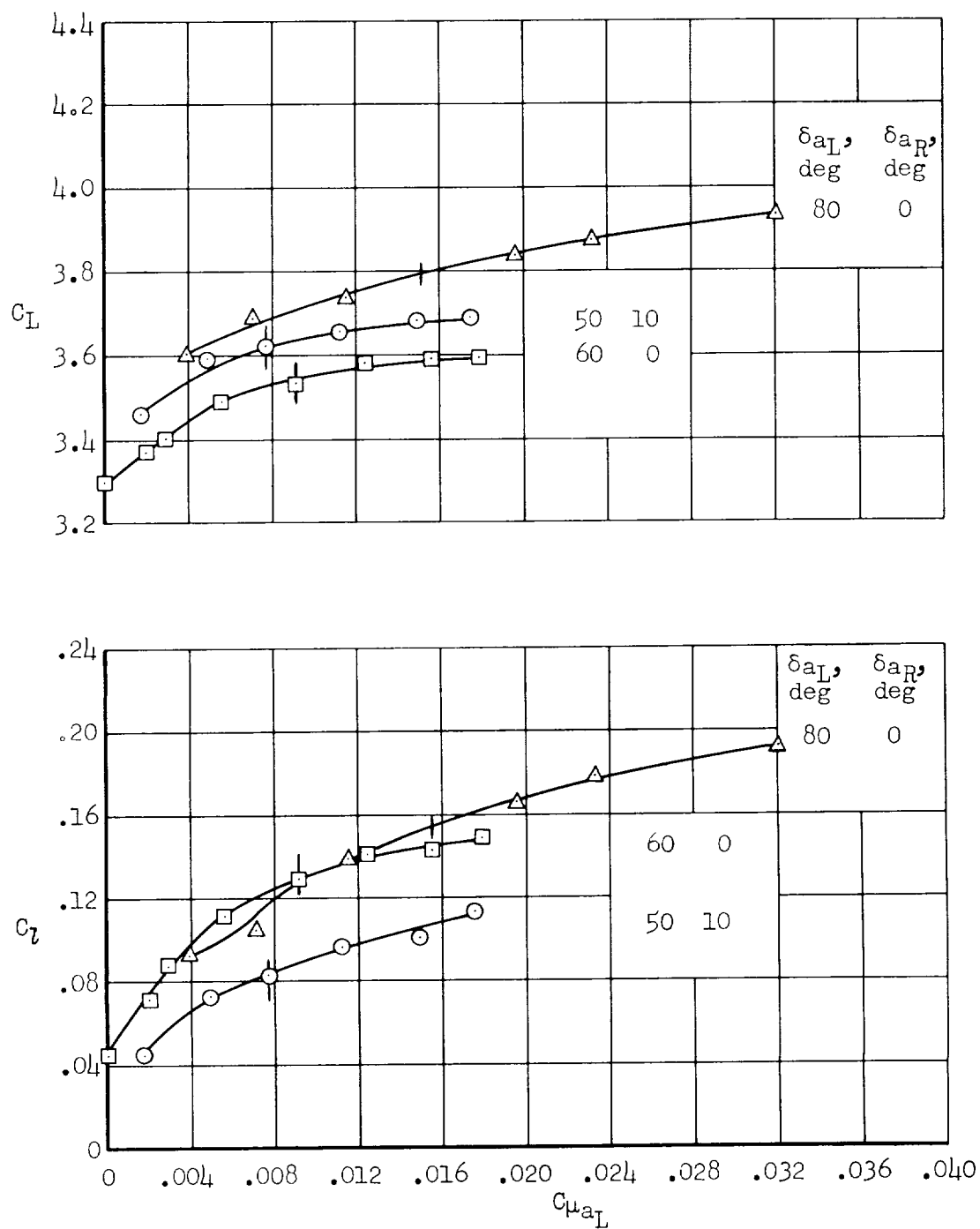


Figure 18.- Variation of lift coefficient and rolling-moment coefficient with left aileron jet momentum coefficient; $C_{\mu_{aR}} = 0$, $\delta_f = 60^\circ$, $C_{\mu_f} = 0.035$, $T_C' = 1.15$, $\alpha_u = 0^\circ$.

<p>NASA MEMO 12-3-58A</p> <p>National Aeronautics and Space Administration.</p> <p>LARGE-SCALE WIND-TUNNEL TESTS OF AN AIRPLANE MODEL WITH AN UNSWEPT, ASPECT-RATIO-10 WING, TWO PROPELLERS, AND BLOWING FLAPS. Roy N. Griffin, Jr., Curt A. Holzhauser, and James A. Weiberg. December 1958. 47p. diags., photo., tab. (NASA MEMORANDUM 12-3-58A)</p> <p>An investigation was made to determine the lifting effectiveness and flow requirements of blowing boundary-layer control applied to a propeller-driven airplane. The blowing prevented flow separation on the flaps and increased the flap lift increment for flap deflections up to the maximum tested of 80°. The effect of the propeller slipstream was to increase the lift increment due to flap deflection. The blowing jet momentum coefficient required for attached flow on the flaps was unaffected by the propeller slipstream.</p> <p>Copies obtainable from NASA, Washington</p>	<ol style="list-style-type: none"> 1. Flaps, Trailing-Edge - Complete Wings (1.2.2.3.1) 2. Boundary-Layer Control - Complete Wings (1.2.2.8.2) 3. Slipstream - Propellers (1.5.4) <ol style="list-style-type: none"> I. Griffin, Roy N., Jr. II. Holzhauser, Curt A. III. Weiberg, James A. IV. NASA MEMO 12-3-58A 	<p>NASA MEMO 12-3-58A</p> <p>National Aeronautics and Space Administration.</p> <p>LARGE-SCALE WIND-TUNNEL TESTS OF AN AIRPLANE MODEL WITH AN UNSWEPT, ASPECT-RATIO-10 WING, TWO PROPELLERS, AND BLOWING FLAPS. Roy N. Griffin, Jr., Curt A. Holzhauser, and James A. Weiberg. December 1958. 47p. diags., photo., tab. (NASA MEMORANDUM 12-3-58A)</p> <p>An investigation was made to determine the lifting effectiveness and flow requirements of blowing boundary-layer control applied to a propeller-driven airplane. The blowing prevented flow separation on the flaps and increased the flap lift increment for flap deflections up to the maximum tested of 80°. The effect of the propeller slipstream was to increase the lift increment due to flap deflection. The blowing jet momentum coefficient required for attached flow on the flaps was unaffected by the propeller slipstream.</p> <p>Copies obtainable from NASA, Washington</p>	<ol style="list-style-type: none"> 1. Flaps, Trailing-Edge - Complete Wings (1.2.2.3.1) 2. Boundary-Layer Control - Complete Wings (1.2.2.8.2) 3. Slipstream - Propellers (1.5.4) <ol style="list-style-type: none"> I. Griffin, Roy N., Jr. II. Holzhauser, Curt A. III. Weiberg, James A. IV. NASA MEMO 12-3-58A 	<p>NASA</p>
<p>NASA MEMO 12-3-58A</p> <p>National Aeronautics and Space Administration.</p> <p>LARGE-SCALE WIND-TUNNEL TESTS OF AN AIRPLANE MODEL WITH AN UNSWEPT, ASPECT-RATIO-10 WING, TWO PROPELLERS, AND BLOWING FLAPS. Roy N. Griffin, Jr., Curt A. Holzhauser, and James A. Weiberg. December 1958. 47p. diags., photo., tab. (NASA MEMORANDUM 12-3-58A)</p> <p>An investigation was made to determine the lifting effectiveness and flow requirements of blowing boundary-layer control applied to a propeller-driven airplane. The blowing prevented flow separation on the flaps and increased the flap lift increment for flap deflections up to the maximum tested of 80°. The effect of the propeller slipstream was to increase the lift increment due to flap deflection. The blowing jet momentum coefficient required for attached flow on the flaps was unaffected by the propeller slipstream.</p> <p>Copies obtainable from NASA, Washington</p>	<ol style="list-style-type: none"> 1. Flaps, Trailing-Edge - Complete Wings (1.2.2.3.1) 2. Boundary-Layer Control - Complete Wings (1.2.2.8.2) 3. Slipstream - Propellers (1.5.4) <ol style="list-style-type: none"> I. Griffin, Roy N., Jr. II. Holzhauser, Curt A. III. Weiberg, James A. IV. NASA MEMO 12-3-58A 	<p>NASA MEMO 12-3-58A</p> <p>National Aeronautics and Space Administration.</p> <p>LARGE-SCALE WIND-TUNNEL TESTS OF AN AIRPLANE MODEL WITH AN UNSWEPT, ASPECT-RATIO-10 WING, TWO PROPELLERS, AND BLOWING FLAPS. Roy N. Griffin, Jr., Curt A. Holzhauser, and James A. Weiberg. December 1958. 47p. diags., photo., tab. (NASA MEMORANDUM 12-3-58A)</p> <p>An investigation was made to determine the lifting effectiveness and flow requirements of blowing boundary-layer control applied to a propeller-driven airplane. The blowing prevented flow separation on the flaps and increased the flap lift increment for flap deflections up to the maximum tested of 80°. The effect of the propeller slipstream was to increase the lift increment due to flap deflection. The blowing jet momentum coefficient required for attached flow on the flaps was unaffected by the propeller slipstream.</p> <p>Copies obtainable from NASA, Washington</p>	<ol style="list-style-type: none"> 1. Flaps, Trailing-Edge - Complete Wings (1.2.2.3.1) 2. Boundary-Layer Control - Complete Wings (1.2.2.8.2) 3. Slipstream - Propellers (1.5.4) <ol style="list-style-type: none"> I. Griffin, Roy N., Jr. II. Holzhauser, Curt A. III. Weiberg, James A. IV. NASA MEMO 12-3-58A 	<p>NASA</p>

